Dear Referee,

Thank you very much for reviewing our manuscript.
Please see the revised manuscript at the end of this document.

General comments:

We rewrote and restructured the whole manuscript. Only a few sentences remained from the original discussion paper.

Additionally we:
- included research from 2015
- included the effect of clouds and the zenith angle of the sun (see Section 2.5.1 and 2.5.2, 2.6)
- improved the transmissivity parameterization (Section 2.8)
- reduced the number of free parameters from six to five (Section 2.10)
- use updated data of the atmospheric input rates of dust and BC (Section 2.11)
- added a discussion Section dealing with assumptions and uncertainties (Section 4.1)
- added a discussion Section about the role of melt-out of impurities (Section 4.2)
- changed the title to: "Albedo reduction of ice caused by dust and black carbon accumulation from melt-out and atmospheric deposition" in order to emphasise the focus on ice and impurity accumulation
- prepared completely new supplementary figures
- changed the unit of the specific surface area to cm^2/g
- redid the Monte Carlo process

Comments
Referee comments are repeated in red.

1) Bad language. Very many sentences are poorly written or grammatically and logically incorrect, showing not only careless in writing, but also lack of clarity of the expressed concepts.

We completely restructured and rewrote the whole manuscript. It was definitely due to poor writing that both reviewers missed the novelty and significance of the manuscript. Therefore, we state them here explicitly and it should be clear by reading the revised manuscript.

novelty: We developed the first model of impurity accumulation on the ice surface the snowpack and its impact on the albedo of ice and melt. In addition we investigated the amount of melt-out of dust and BC versus atmospheric input, which to our knowledge has not been done before.
significance: The presented framework can be used to study the long-term effect of dust and BC on future melt and sea level rise. It has already been used in Goelles et al. 2015, which has more than 880 views and downloads since its publication on the 22nd of September and got mainstream news coverage (checked on 26.01.2016).

Here are few examples:
p. 1348, lines 12-15: "Sophisticated snow albedo model like SNICAR (Flanner and Zender, 2006) have existed for some time. While these models are computationally to demanding to include in large scale models they give important insight to efficient parameterizations (Pirazzini, 2009)". Do the authors mean the model SNICAR efficiently parameterize the quantities that control the snow albedo? In fact, SNICAR is currently applied in several climate and numerical weather prediction models as its computational cost is very limited. However, SNICAN cannot be implemented into those simple models that have a single snow layer.

This paragraph has been deleted from the new version of the manuscript.

p. 1354, line 1: "The basic method for snow and ice albedo are the same . . .". Do the authors mean that the method to account of the impact of impurities on albedo is the same for snow and ice?

Yes, the methods of Gardner and Sharp are valid for both snow and ice. This sentence has been deleted in the revised manuscript and the equations for snow and ice are explicitly mentioned.

p. 1355, lines 19-21: "In this study we focus mainly on ice albedo and therefore left the snow albedo is defined by differentiating between wet and dry snow as in Robinson et al. (2010) although the model includes also snow albedo reduction due to BC and dust". This confused sentence leaves totally unclear how snow albedo is treated in the study.

We now state our design goal of the model explicitly in the introduction, and this sentence has been deleted.

The new paragraph from the introduction:
"We present the first SMB model which takes the effect of impurity accumulation on ice albedo into account. The ice albedo is part of the surface albedo scheme which includes the seasonal change between snow and ice surface. The design goal for the model is that it can be used as an alternative to positive degree day models, which are widely used in standalone ice sheet and glacier models. The model framework is applied and tested on the western margin of the GrIS. "

The paper is far from being adequate for scientific publication and needs to be completely rewritten by a scientist who is fluent in English.

As mentioned above, we rewrote and reorganised the manuscript completely with external help.

2) The method applied in the study is not rigorous and cannot be accepted. First of all, all the equations introduced in Sections 2.2, 2.3, 2.4 and 3.3 are quite rough and con- sist of simple parameterizations of complex physical processes. They can be applied only if their uncertainties are properly estimated. As the developed model aims to give quantitative estimations of aerosol impact on albedo reduction, an accurate assessment of the model uncertainties is mandatory. In fact, the large variability of the fitting parameters among different years tells that the model is oversimplified and completely inadequate for quantitative estimations. Secondly, many of the equations (6, 7, 8, 11) are given without referring to the source, and without explaining the reasoning behind their choice or development.

The reasons why we choose the simplified energy balance are given in the Section 2.1 of the revised manuscript. The equations in the SMB Section (originally Section 2.2), melt (originally Section 2.3) and surface albedo (originally Section 2.3) are all based on Robinson et al., 2010. The uncertainties of those model components are described in detail in the paper Fitzgerald et al. (2012). Which is now mentioned in the first paragraph in Section 4.1. The uncertainties of the other components are also discussed in Section 4.1, including the temperature and precipitation parameterization (originally Section 3.3).

Comments concerning missing references of equations:
.) Equation 6 (now 3) is from (Robinson et al., 2010)
.) The reference of equation 7 has been given before (Bales et al., 2009; Calanca et al., 2000) (Line 2 on Page 1352)
.) Equation 8 (now 22) is also from (Robinson et al., 2010)
.) Equation 11 (now 18) is based on Van den Berg et al. (2008) and Robinson et al. (2010), which has been mention in the original version of the manuscript (line 19 on page 1353)

The process of "validation" was not well introduced in the original manuscript. The "validation" is now described in the new Section 2.10 "Calibration and evaluation". In short: the calibration uses data of one year and the calibrated model is then used over to simulate the whole period. Then the result is compared to the remaining part of the dataset, which were not used in the calibration. This process is similar to "cross-validation" of statistical models. Where the model is "trained" on data of one year and afterwards the model is tested on the remaining dataset.

In the revised manuscript we wrote:
"The calibration period of one season makes it possible to calibrate and evaluate the model on the same dataset. The model is calibrated on data of one year and then applied to the remaining period. This makes it possible to investigate the variability of the free parameters."

In addition the parameter set of KAN_M was applied to Station S5, which demonstrates the spatial applicability of the model. The parameter set obtained from the calibration at KAN_M in the year 2010 performs well at both stations.

3) Some of the utilized quantities are not properly defined: for instance, what is Ms obtained via Eq. (9)? At p.1355, line 1 the authors write that "the active fraction Fice,n describes the fact that not all impurities are influencing the albedo". Does it mean that the active fraction is the fraction of aerosol that contributes to the reduction of ice albedo? Also, on p. 1355 lines 14-15 the authors describe the "effective depth" as "re- lated to the absorption length in ice which is depending on wavelength and impurities". What is then the effective depth, the penetration depth of light into the ice at a specific wavelength and impurity content??

Ms is the potential melt rate, as mentioned in Line 15 on page 1351 in the first version. It is now explicitly mentioned before the equation (Eqn. 19).

Yes, the active fraction is the fraction of aerosols which contributes to ice albedo reduction. This is now mention after the equation (Eqn. 12). The new sentence reads:
"… where only the active fraction F contributes to the ice albedo reduction. A value of one means that all impurities are dispersed on the ice surface and therefore all impurities reduce the ice albedo directly. "

The effective depth is the penetration depth of light into clear ice with an extinction coefficient of 1.6 m^−1. See the new text:
"…where d_{eff} is the effective depth (in meters). This assumes that impurities on the ice surface have an equivalent effect as the same amount of impurities uniformly distributed in the ice over the effective depth. The effective depth is derived from the extinction coefficient of ice. Less than one permille of the original energy remains at a depth of 5 meters clear white ice with an extinction coefficient of 1.6 m^{-1} (Bøggild et al., 1995). "

4) The authors state that their study focuses mainly on the ice albedo (p. 1355, line 19), but for a large fraction of their considered period (April-September) the ice surface is covered by snow. Thus, from the point of view of surface energy and mass balance, the effect of impurity on snow albedo is equally or more important as the effect of impurities on ice albedo. The authors should study and eventually apply the research done in this field. Some recent publications are:

a. Oaida, C. M., Y. Xue, M. G. Flanner, S. M. Skiles, F. De Sales, and T. H. Painter (2015), Improving snow albedo processes in WRF/SSi regional climate model to as- sess impact of dust and black carbon in snow on surface energy balance and hydrol- ogy over western U.S., J. Geophys. Res. Atmos., 120,doi:10.1002/2014JD022444.

b. Kokhanovsky, A. (2013), Spectral reflectance of solar light from dirty snow: a simple theoretical model and its validation, The Cryosphere, 7, 1325–1331.

c. Dang, C., R. E. Brandt, and S. G. Warren (2015), Parameterizations for narrowband and broadband albedo of pure snow and snow containing mineral dust and black carbon, J. Geophys. Res. Atmos., 120, doi:10.1002/2014JD022646.

We choose to focus on ice albedo, because there are already many studies on the albedo of snow, as for example to once in your list. Yes, eventually the snow albedo can and will be included, and is of course important for the overall SMB of the Greenland ice sheet. In this study the focus is on ice albedo and the ablation zone, which is also reflected in the new title and introduction and throughout the revised manuscript.

Here are other reasons why we treaded snow albedo the way we did.

1.) Due to the design goal we wanted to have as little input variables and parameters as possible. Therefore, we chose a constant precipitation parameterization and a simplified energy balance. This makes it impossible to account for individual snowfall events and therefore grain growth. Grain growth is only indirectly included by distinguishing between wet and dry snow. Grain growth of snow has by far the biggest effect on the albedo of snow on the Greenland ice sheet and the effects of BC and dust are comparably small, as can be seen in the new Figure S2 in the supplements. Even for very dense snow and very high concentrations of BC and dust (for Greenland), the overall effect of impurities is less than 0.06 (see also Figure S2). Therefore, it is necessary to treat the grain growth adequately first, before including the effect of impurities on snow. In addition the effect of impurities on snow albedo depends on the specific surface area which is also liked to grain sizes.
We are fully aware that this is a limitation, and it is mentioned throughout the revised manuscript. In future versions of the model the snowpack and snow albedo components can be replaced by any of your mentions studies or others.

2.) The major share of meltwater production at the K-transect is caused by ice melt. Because the annual mean accumulation is around 0-0.18 meters of water equivalent (Burgess et al. 2010), while ice melt is in the order of meters and up to 5 meters water equivalent per year.

3.) Ice is exposed when solar radiation is at its maximum. The radiation is low when the seasonal snow cover is intact in spring and autumn.

4.) The effect of impurities on ice is bigger than on snow because of the lower specific surface area of ice (see Figure S2 in the supplements). In addition, the amount of impurities on ice are higher because of accumulation over several years and the additional large source of impurities from melt-out.

5.) The time-span and areal extend of exposed ice will increase under a warmer climate in the future (Box et al. 2012, Tedesco et al. 2011) due to a rising equilibrium line and earlier onset of melt caused by higher temperatures. Therefore, the influence of ice albedo will increase in the future.

Nevertheless, it is certainly desirable to improve the snow albedo in the future, in order to improve the SMB and the timing of ice exposure.

Extra comments

Yes it might be rare, but the parameterization should not rule it out.
We included the sentence: "This equation allows the snow albedo to be lower than the ice albedo, which could be the case, although rare, when debris rich wet snow covers clean ice.

It includes the "active fraction" and the englacial concentration (see Equation 12 and Section 2.5 in the new manuscript).

The stations were named by GEUS and IMAU and we included information of the correct station names in the caption of the Figure (now Figure 1).

Sincerely,
T. Goelles and C. E. Bøggild

References

Box, J. E., Fettweis, X., Stroeve, J. C., Tedesco, M., Hall, D. K. and Steffen, K.: Greenland ice sheet albedo feedback: thermodynamics and atmospheric drivers, The Cryosphere, 6(4), 821–839, doi:10.5194/tc-6-821-2012, 2012.

Burgess, E. W., Forster, R. R., Box, J. E., Mosley-Thompson, E., Bromwich, D. H., Bales, R. C. and Smith, L. C.: A spatially calibrated model of annual accumulation rate on the Greenland Ice Sheet (1958–2007), Journal of Geophysical Research, 115(F2), F02004, doi: 10.1029/2009JF001293, 2010.

Goelles, T., Bøggild, C. E. and Greve, R.: Ice sheet mass loss caused by dust and black carbon accumulation, The Cryosphere, 9(5), 1845–1856, doi:10.5194/tc-9-1845-2015, 2015.

Tedesco, M., Fettweis, X., Van den Broeke, M. R., Van de Wal, R. S. W., Smeets, C. J. P. P., Van de Berg, W. J., Serreze, M. C. and Box, J. E.: The role of albedo and accumulation in the 2010 melting record in Greenland, Environ. Res. Lett., 6(1), 014005, doi:10.1088/1748-9326/6/1/014005, 2011.

Van As, D., Hubbard, A. L., Hasholt, B., Mikkelsen, A. B., Van den Broeke, M. R. and Fausto, R. S.: Large surface meltwater discharge from the Kangerlussuaq sector of the Greenland ice sheet during the record-warm year 2010 explained by detailed energy balance observations, The Cryosphere, 6(1), 199–209, doi:10.5194/tc-6-199-2012, 2012.

Van de Wal, R. S. W., Boot, W., Smeets, C., Snellen, H., Van den Broeke, M. R. and Oerlemans, J.: Twenty-one years of mass balance observations along the K-transect, West Greenland, Earth System Science Data, 4, 31–35, doi:10.5194/essd-4-31-2012, 2012.

Albedo reduction of ice caused by dust and black carbon accumulation from melt-out and atmospheric deposition

T. Goelles[1,2] and C. E. Bøggild[3]

[1]The University Centre in Svalbard (UNIS), Longyearbyen, Norway
[2]Norwegian University of Life Sciences (NMBU), Aas, Norway
[3]Arctic Technology Centre, Technical University of Denmark, Kgs. Lyngby, Denmark

Correspondence to: T. Goelles (thomas.golles@unis.no, thomas.goelles@gmail.com)

Abstract. Surface melt in the ablation zone is controlled by atmospheric temperature and surface albedo. Impurities accumulate on the ice surface and lower the albedo of ice. Non-biological impurities, such as mineral dust and black carbon (soot), accumulate by dry or wet deposition and by melt-out. The darkening effect of accumulating impurities on the ice surface is currently not included in surface mass balance models and sea level projections. We present a model framework which includes impurity melt-out and accumulation, the effect of clouds and the angle of the sun on albedo and ultimately surface mass balance. The main source of dust on the ice surface is melt-out from dust deposited during glacial periods, whereas current atmospheric deposition contributes insignificantly. While for black carbon the atmospheric deposition dominates at melt rates below one meter. Runoff of impurities is in the range of one permille per day, which leads to a residence time of decades on the ice surface in which the albedo is lowered and melt is enhanced.

1 Introduction

The increased mass loss of the Greenland ice sheet (GrIS) since 2009 is mainly caused by an increase in surface melt and runoff (Enderlin et al., 2014). Surface melt is largely determined by the amount of absorbed shortwave radiation (Van den Broeke et al., 2008), which is governed by the surface albedo. Hence, the broadband albedo (from now on just referred to as albedo) has been identified as a major component of the surface mass balance (SMB) of the GrIS (Bougamont et al., 2005; Tedesco et al., 2011; van Angelen et al., 2012).

The broadband albedo of ice varies highly over space and time (e.g. Bøggild et al., 2010; Chandler et al., 2015), but in most model studies ice albedo is still treated as a uniform constant (e.g. Mernild et al., 2010; Rae et al., 2012) or as constant over time (e.g. Noël et al., 2015). Snow albedo, on the other hand, is often modeled by multi-layer snowpack and radiative transfer models, considering grain growth and impurities (e.g. Gent et al., 2011; Lipscomb et al., 2013; Oaida et al., 2015). Models of ice albedo are still at their infancy.

25   The highest melt rates of the GrIS are observed in the ablation area, where ice is exposed at some point of the year, after the seasonal snow has disappeared. This goes in hand with a drop in surface albedo because the albedo of ice is significantly lower than that of snow (e.g. Moustafa et al., 2015). The duration and area of exposed ice will increase under a warmer climate (Brutel-Vuilmet et al., 2013; Vizcaino et al., 2014) as snow melts earlier and the equilibrium line moves to higher

30   elevations. Therefore, the role of ice albedo on surface melt of the GrIS, and ultimately sea level rise, will increase in the future.

We present the first SMB model which takes the effect of impurity accumulation on ice albedo into account. The ice albedo is part of the surface albedo scheme which includes the seasonal change between snow and ice surface. The design goal for the model is that it can be used as an alternative

35   to positive degree day models, which are widely used in standalone ice sheet and glacier models. The model framework is applied and tested on the western margin of the GrIS.

First we begin with an outline of impurities on snow and ice, and the description of the model test site. In Section 2 we present the model equations and parameters, and the calibration procedure, followed by model results. We conclude by discussing the result of model simulations at two locations

40   and the role of impurity melt-out.

1.1 Albedo and impurities

Absorption of ice at visible wavelengths is very weak, therefore small amounts of highly absorbent impurities have a big effect on snow and ice albedo (Wiscombe and Warren, 1980; Warren and Wiscombe, 1980; Warren and Brandt, 2008). The most absorbent impurity is black carbon (BC),

45   which is about 200 times more absorbent than mineral dust (Dang et al., 2015). BC particles are highly absorptive in the visual range, where the solar radiation is greatest. In addition to the aerosols dust and BC, microbes may influence the albedo by aggregating material (Takeuchi et al., 2001) and by production of dark materials (Takeuchi, 2002; Remias et al., 2012). Brown-black ice algae can potentially decrease the albedo of ice by up to 40 percent relative to clean ice (Yallop et al., 2012).

50   Despite the potentially high influence of microbes, their dynamics and exact effect on albedo are not well understood (Stibal et al., 2012; Yallop et al., 2012).

Non-biological impurities on the ice surface accumulate by dry or wet deposition, by release of impurities in the snowpack or by melt-out of englacial impurities. The ice itself acts as a reservoir of mineral dust and BC (Reeh et al., 1991; Bøggild et al., 1996). These englacial impurities travel with

55   the ice towards the ablation zone where they melt-out and contribute to the impurity mass on the ice surface (e.g. Oerlemans, 1991; Bøggild et al., 1996; Klok and Oerlemans, 2002; Oerlemans et al., 2009). The accumulated impurities on the ice surface lower the albedo for several years, because they are preserved under the winter snow cover, and re-emerge in spring.

The effect of impurities on snow, on the other hand, is short. A substantial snowfall in winter

60   resets the snow albedo to the high values of fresh dry snow (Dumont et al., 2014). In spring, when

2

snow melts, the impurities tend to concentrate at the snow surface which amplifies the impact of impurities on snow albedo (Doherty et al., 2010, 2013). However, the impact at the ablation zone is still rather short because the snow cover is thin and therefore the period of snow melt is short. After all snow has melted the impurities of the snowpack are released onto the ice surface.

65 Typical values of BC in snowpack are around $3 \, \mathrm{ng \, g^{-1}}$ with peaks of $20 \, \mathrm{ng \, g^{-1}}$ (Dumont et al., 2014). Values of dust concentration in snow can reach up to $500 \, \mathrm{ng \, g^{-1}}$ (Dumont et al., 2014), which has about the same effect on albedo as $2.5 \, \mathrm{ng \, g^{-1}}$ BC. Dust concentration in ice cores are up to 9000 $\mathrm{ng \, g^{-1}}$ Ruth et al. (2003) and of BC up to $16 \, \mathrm{ng \, g^{-1}}$ McConnell et al. (2007). While the surface concentration of Impurities on ice range from $16 \, \mathrm{g \, m^{-2}}$ up to $1.4 \, \mathrm{kg \, m^{-2}}$ (Bøggild et al., 2010).

1.2 The K-transect in western Greenland

The so-called "K-transect" (also known as Søndre Strømfjord transect) is located on the western margin of the GrIS at $67°\,\mathrm{N}$ (Fig. 1) and has been the target of numerous field campaigns. We chose this location as the test site for the model because of available SMB measurements as well as continuous automatic weather station observations.

75 Accumulation in the K-transect is low compared to other parts of the GrIS (Burgess et al., 2010). At low elevation near station S5 snow is redistributed by wind into gullies and crevasses (Van den Broeke et al., 2008), causing ice exposure throughout the melting season. While at higher stations up to Station S9, near the equilibrium line, ice is covered by snow in the beginning of the melt season and exposed later on.

80 It is also an interesting area because a "dark region" persists below the equilibrium line each melt season. The region is about $30 \, \mathrm{km}$ wide and starts at approximately $30 \, \mathrm{km}$ away from the margin (Wientjes and Oerlemans, 2010). Previously the cause of this dark region was believed to be meltwater (Zuo and Oerlemans, 1996), but now is attributed to dust (Wientjes and Oerlemans, 2010) and carbonaceous particles (Wientjes et al., 2012). This dark area, the available data and the 85 ice exposure makes the K-transect an ideal test location for our model.

2 Model description

2.1 Model framework and setup

A full surface energy balance model is not feasible because it requires information about winds, cloud cover, relative humidity, etc. which are not available in standalone ice sheet models. Therefore, 90 the centerpiece of the SMB model is a simplified energy balance which takes albedo into account. Our model framework consists of seven components shown in Figure 2 and the common parameters are listed in Table 1. The *temperature and precipitation parameterization* and *impurity accumulation* components are our own developments, the snow and ice albedo component are largely based on Gardner and Sharp (2010), and the other components are based on Robinson et al. (2010).

3

95   The model simulates surface albedo, impurity loadings, snow thickness and SMB for one square meter on an ice sheet or glacier. It is realized in Mathematica (version 10, Wolfram Research, Inc., 2014) using self-coded solvers for the differential equations, with a time-step of one day. The following sections describe each component in the order of the flow chart.

2.2 Temperature and precipitation parameterization

100 The near-surface temperatures at the ablation zone of GrIS are stable during the summer months due to the cooling effect of melting ice. Therefore, temperatures are stable during the summer and fluctuate during the winter months. Hence, we did not use a sinusoidal parameterization, which is normally used (e.g. Reeh, 1991), but a trapezoid shape:

$$
T = \begin{cases} T_\oplus & t_{\odot,\text{start}} \le t \le t_{\odot,\text{end}} \\ t \cdot \varsigma - t_{\odot,\text{start}} \cdot \varsigma + T_\oplus & t < t_{\odot,\text{start}} \\ -t \cdot \varsigma + t_{\odot,\text{end}} \cdot \varsigma + T_\oplus & t > t_{\odot,\text{end}} \end{cases} \tag{1}
$$

105   where $T_\oplus$ is the mean of all temperatures above $0\,^\circ\text{C}$. The first day of the summer $t_{\odot,\text{start}}$ is set to May 1 and the last day with positive temperatures $t_{\odot,\text{end}}$ is set to September 1. The non-summer temperatures are defined by the slope ς in $^\circ\text{C}$ per day when the time t is in days. This parameterization of the negative temperatures is sufficient because melt is unaffected by them.

    The precipitation rate is parameterized by the annual mean precipitation rate $P = \overline{P}$. This is jus-

110 tifiable because the snow depth is unaffected by high frequency fluctuations of precipitation. The disadvantage of this simple parameterization is that it makes it impossible to resolve individual snowfall events. Therefore, it is also impossible to account for snow grain growth as well as summer snowfall.

2.3 Snowpack

115 Snow depth (d) is required for the final SMB, and in order to distinguish between snow and ice surface. It is calculated by a balance between solid precipitation rate P_{solid} and melt rate M_{s} (Robinson et al., 2010):

$$
\frac{\text{d}}{\text{d}t}d = P_{\text{solid}} - M_{\text{s}}, d \in (0, d_{\text{max}}) \tag{2}
$$

    If the snow depth exceeds $d_{\text{max}} = 5\,\text{m w.e.}$ (Robinson et al., 2010; Fitzgerald et al., 2012) the snow

120 depth is reset to 5 meters and the surplus amount is added to the ice thickness. This accounts for the snow to ice metamorphism in the accumulation zone. The solid precipitation rate P_{solid} in Eq. (2) depends on a temperature-dependent fraction $f(T)$ and the total precipitation rate P (Robinson et al., 2010):

$$P_{\text{solid}} = P \cdot f(T) \tag{3}$$

where the surface temperature-depending fraction $f(T)$ is empirically based on data of Greenland (Bales et al., 2009; Calanca et al., 2000) and states that below a minimum temperature ($T_{\min} = -7\,^{\circ}\text{C}$) all precipitation is snow and above a maximum temperature ($T_{\max} = +7\,^{\circ}\text{C}$) rain:

$$f(T) = \begin{cases} 1 & T < T_{\min} \\ 0 & T > T_{\max} \\ \cos\left(\frac{T - T_{\min}}{T_{\max} - T_{\min}}\right)\left(\frac{\pi}{2}\right) & T_{\min} < T < T_{\max} \end{cases} \tag{4}$$

2.4 Impurity accumulation

Particulate impurities such as BC and mineral dust as well as microbes have four different sources (Fig. 3):

- *atmosphere – distant sources*: (k_{I}) by dry or wet deposition,

- *atmosphere – local sources*: (k_{II}) by regionally transported material from the surrounding tundra,

- *flow*: (k_{III}) by transport from the accumulation zone to the ablation zone where impurities melt-out,

- *biological*: (k_{IV}) by local biological production of dark material on the ice or snow surface.

The contribution of each of these sources is different for each impurity species. Where the biological source k_{IV} is only relevant for microbes. Organic matter was found to contribute only about 5 percent to the impurity mass on the ablation zone of the GrIS (Bøggild et al., 2010; Wientjes et al., 2011; Takeuchi et al., 2014). Because of the comparably low concentrations of organic matter and its unknown absorption we omit microbes for now, but prepare the impurity accumulation in a way that it can be included in the future.

The atmospheric sources (k_{I} and k_{II}) contribute to BC and dust accumulation both in the ice sheet interior and at the margin. While the melt-out of englacial impurities, source k_{III}, only contributes in the ablation zone when ice melts. The following equations are valid for both BC (n=BC) and dust (n=dust).

Both atmospheric sources contribute directly to the impurity mass inside the snowpack $\iota_{\text{snow,n}}$ ($\text{ng}\,\text{m}^{-2}$) as well as the local biological production. We assume that impurities stay within the snowpack once they are inside. Therefore, the impurity concentration inside the snowpack is described by:

$$\frac{\mathrm{d}\iota_{\mathrm{snow,n}}}{\mathrm{d}t} = \begin{cases} k_{\mathrm{I,n}}(t) + k_{\mathrm{II,n}}(t) + k_{\mathrm{IV,n}}(t) & d > 0 \\ 0 & d = 0 \end{cases} \tag{5}$$

As ice is exposed (snow depth $d = 0$) englacial impurities as well as the atmospheric sources and local production all contribute to the impurity mass on the ice surface $\iota_{\mathrm{ice,n}}$ ($\mathrm{ng\,m^{-2}}$). The impurity accumulation is counteracted by a reduction term ($r_{\mathrm{ice}}(t)\,\iota_{\mathrm{ice,n}}$), which describes removal by meltwater and is assumed to be the same for dust and BC. We assume no resuspension of impurities, because the surface on which they reside is either wet or frozen. Further, we assume that once the snow cover disappears all the impurities in the snowpack get instantly added to the impurity content of the ice surface and no impurity flux from the ice towards the snowpack:

$$\frac{\mathrm{d}\iota_{\mathrm{ice,n}}}{\mathrm{d}t} = \begin{cases} 0 & d > 0 \\ k_{\mathrm{I,n}}(t) + k_{\mathrm{II,n}}(t) + k_{\mathrm{III,n}}(t) + \\ \quad + k_{\mathrm{IV,n}}(t) - r_{\mathrm{ice}}(t)\iota_{\mathrm{ice,n}} & d = 0 \end{cases} \tag{6}$$

The contribution of melt-out of englacial impurities $k_{\mathrm{III,n}}(t)$, which are transported by ice flow, depends on the melt rate of ice and the englacial impurity concentration $[\iota_{\mathrm{englacial,n}}]$ (in $\mathrm{ng\,g^{-1}}$ or ppb). We assume that the impurity content in superimposed ice ($h_{\mathrm{s.ice}}$) is 0, since observations indicate a very small impurity concentration in superimposed ice (Chandler et al., 2015) and impurities accumulate on the snow surface as it melts:

$$k_{\mathrm{III,n}}(t) = \begin{cases} [\iota_{\mathrm{englacial,n}}]1000\frac{\mathrm{d}h_{\mathrm{ice}}}{\mathrm{d}t}\rho_{\mathrm{ice}} & h_{\mathrm{s.ice}} = 0 \\ 0 & h_{\mathrm{s.ice}} > 0 \end{cases} \tag{7}$$

in $\mathrm{ng\,m^{-2}}$ and where h_{ice} is the thickness of ice (see 2.9) and ρ_{ice} is the density of ice in $\mathrm{kg\,m^{-3}}$.

2.5 Ice albedo

The ice albedo depends on its specific surface area $\hat{S}$, the effect of impurities ($\mathrm{d}\alpha_{\mathrm{c}}$), the zenith angle of the sun ($\mathrm{d}\alpha_{\theta_z}$) and the effect of clouds ($\mathrm{d}\alpha_{\mathrm{clouds}}$). Gardner and Sharp (2010) developed a parameterization based on experiments with a radiative transfer model of snow and ice coupled to a similar model of the atmosphere:

$$\alpha_{\mathrm{ice}} = \alpha_{\hat{S}} + \mathrm{d}\alpha_{\mathrm{c}} + \mathrm{d}\alpha_{\theta_z} + \mathrm{d}\alpha_{\mathrm{clouds}} \tag{8}$$

Where $\alpha_{\hat{S}}$ is the albedo of clean ice with a zenith angle of 0 and no clouds. It is is determined by the specific surface area $\hat{S}$ in $\mathrm{cm^2\,g^{-1}}$, which depends on the size and distribution of air bubbles and cracks (Gardner and Sharp, 2010):

$$\alpha_{\hat{S}} = 1.48 - \hat{S}^{-0.07} \tag{9}$$

The albedo reduction due to BC is modeled by the equation (Gardner and Sharp, 2010):

$$d\alpha_c = \max\left(0.04 - \alpha_{\hat{S}}, \frac{-c^{0.55}}{0.16 + 0.6\,\hat{S}^{0.5} + 1.8\,c^{0.6}\,\hat{S}^{-0.25}}\right) \tag{10}$$

which is designed for concentrations of BC (c in ppmw) and the effect of dust can be included by adding an BC equivalent term. We use a scaling factor of 1/200 to account for the lower absorption of dust (Gardner and Sharp, 2010; Dang et al., 2015). We define an effective concentration of BC and dust, which accounts for both englacial impurities and impurities located on the ice surface:

$$c = [\iota_{\text{eff,BC}}] + [\iota_{\text{eff,dust}}] \cdot 1/200 \tag{11}$$

where $[\iota_{\text{eff,n}}]$ is the effective aerosol concentration in ppmw, which depends on the englacial concentration as well as the *active* component of the impurities located on the ice surface. A certain fraction of impurities can be inside cryoconite holes, and therefore shielded from the low-standing sun (Bøggild et al., 2010). This is expressed by the active fraction $\mathcal{F}$, which is assumed to be the same for BC and dust, in the equation:

$$[\iota_{\text{eff,n}}] = [\iota_{\text{englacial,n}}] + [\iota_{\text{ice,n}}] \cdot \mathcal{F} \tag{12}$$

where only the active fraction $\mathcal{F}$ contributes to the ice albedo reduction. A value of one means that all impurities are dispersed on the ice surface and therefore all impurities reduce the ice albedo directly.

The impurity accumulation on ice (Eqn. 6) is calculated in ng per square meter, while Equation 10 requires the fractions of weight (ppmw). We therefore use the following equation to convert between the two quantities:

$$[\iota_{\text{ice,n}}] = \frac{\iota_{\text{ice,n}}}{\rho_{\text{ice}}\,d_{\text{eff}}}\,10^6 \tag{13}$$

where d_{eff} is the effective depth (in meters). This assumes that impurities on the ice surface have an equivalent effect as the same amount of impurities uniformly distributed in the ice over the effective depth. The effective depth is derived from the extinction coefficient of ice. Less than one permille of the original energy remains at a depth of 5 meters of clear white ice with an extinction coefficient of $1.6\,\text{m}^{-1}$ (Bøggild et al., 1995).

2.5.1 Clouds

Clouds cause a spectral shift in incident radiation which increases the broadband albedo with increasing cloud optical thickness τ. The change of albedo caused by clouds is obtained by (Gardner and Sharp, 2010):

$$d\alpha_{\text{clouds}} = \frac{0.1\tau(\alpha_{\hat{S}} + d\alpha_{\text{c}})^{1.3}}{(1 + 1.5\tau)^{\alpha_{\hat{S}}}} \tag{14}$$

which depends, besides the cloud optical thickness τ, on the specific surface area and the impurity content.

The effective cloud optical thickness at the K-transect varies between 4 and 14 with an annual mean of 9.0 at S5, of 8.4 at S6 and of 8.0 at S9 (Van den Broeke et al., 2008). Hence, the cloud optical thickness decreases with elevation h (in m) and is expressed by (see Figure S1a in the supplements):

$$\tau = 9.45 - 0.001 \cdot h \tag{15}$$

and is constant over the year.

2.5.2 Zenith angle of the sun

Albedo increases with increasing zenith angle because light is less likely to penetrate deep into ice or snow. Hence, the path length is shorter and the albedo is higher. This is parameterized by (Gardner and Sharp, 2010):

$$d\alpha_{\theta_z} = 0.53\alpha_{\hat{S}}(1 - (\alpha_{\hat{S}} + d\alpha_{\text{c}}))(1 - \cos\theta_z)^{1.2} \tag{16}$$

where θ_z is the zenith angle. The influence of the zenith angle is highest in spring and autumn when the zenith angle is high, and is around 0.13. At the same time solar radiation is low and therefore the impact of albedo on melt is also low. In mid-summer the effect at the K-transect is around 0.05 for clean ice and 0.08 for ice with 0.1 ppm BC (see Figure S1b in the supplements). Hence, $d\alpha_{\theta_z}$ is higher with higher impurity loading. Due to the shorter path length it is less likely that solar radiation encounters impurities and therefore the albedo is higher with high zenith angles. Nevertheless, the overall effect of impurities on albedo is still negative, but weakened when the zenith angle is high.

2.6 Snow albedo

We keep snow albedo unaffected by impurities in this study, since the concentrations are low and the effect on surface albedo in the ablation zone is short (see also Figure S2 in the supplements). Other than that, the same equations as for ice are used and the effect of clouds and the zenith angle (Eqn. 14 and 16) are still captured:

8

$$\alpha_{\text{snow}} = \alpha_{\hat{S}} + \text{d}\alpha_{\theta_z} + \text{d}\alpha_{\text{clouds}} \tag{17}$$

The precipitation rate is constant due to the limitations of our design goal. Therefore, individual snowfall events can not be captured. Thus, the effect of grain growth is approximated by two distinct values of $\alpha_{\hat{S}}$ in Equation 17: one for dry snow ($\alpha_{\hat{S}} = \alpha_{\hat{S},\text{ds}}$) and one for wet snow ($\alpha_{\hat{S}} = \alpha_{\hat{S},\text{ws}}$). Wet snow appears if there was melt at the previous time-step.

2.7 Surface albedo

The albedo at a geographical point on a glacier or ice sheet is determined by the surface type, clouds, the solar zenith angle and impurities. If the snow depth is below a critical mark d_{crit} the surface albedo is still influenced by the darker underlaying ice (see Figure 4). Above the critical snow depth d_{crit} the surface albedo is equivalent to the the albedo of α_{snow} (based on Van den Berg et al. (2008); Robinson et al. (2010)):

$$\alpha_s = \begin{cases} \alpha_{\text{ice}} & d = 0 \\ \alpha_{\text{ice}} + \frac{d}{d_{\text{crit}}}(\alpha_{\text{snow}} - \alpha_{\text{ice}}) & 0 < d < d_{\text{crit}} \\ \alpha_{\text{snow}} & d \geq d_{\text{crit}} \end{cases} \tag{18}$$

This equation allows the snow albedo to be lower than the ice albedo, which could be the case, although rare, when debris rich wet snow covers clean ice.

2.8 Potential melt

Many parameterizations of surface melt with different levels of complexity exist, but only a few directly account for albedo. We use a simplified energy-balance model based on Oerlemans (2001) to derive the potential melt rate M_s:

$$M_s = \frac{1}{\rho_w L_m}[\tau_a(1 - \alpha_s)S_{\text{TOA}} + c + \lambda T] \tag{19}$$

where ρ_w is the density of water, L_m is the latent heat of melting, τ_a is the transmissivity, S_{TOA} the insolation on top of the atmosphere, c and λ are empirical parameters, and T is the surface air temperature. The term $c + \lambda T$ is a parameterization of the longwave radiation and turbulent heat flux optimized for Greenland (Robinson et al., 2010, 2011; Fitzgerald et al., 2012).

The term $\tau_a(1 - \alpha_s)S_{\text{TOA}}$ describes the net shortwave radiation and requires only the insolation on top of the atmosphere, which can be calculated for any time and location (Liou, 2002). The transmissivity τ_a is based on net shortwave radiation data and is a linear fit with elevation h in meters:

9

$$\tau_a = 0.56 + 0.00012\,h \tag{20}$$

This equation was derived by comparison of the model net shortwave term $(\tau_a(1-\alpha_s)S_{\text{TOA}})$ with the albedo derived from the AWS data to radiation data (see Figure S3 in the supplements). The resulting transmissivity is higher than the one used by Robinson et al. (2010), which was based on ERA-40 while Eqn. 20 is based on AWS data for the period (2005-2012) for years with complete shortwave radiation data.

2.9 Surface mass balance

The change of ice thickness h_{ice} in m w.e. together with the snow depth forms the SMB component of the model. The equation accounting for refreezing reads (Robinson et al., 2010):

$$\frac{\mathrm{d}}{\mathrm{d}t}h_{\text{ice}} = \begin{cases} M_s r_f & d > 0 \\ \min\left(P_{\text{solid}} - M_s, 0\right) & d = 0 \end{cases} \tag{21}$$

where r_f is the refreezing fraction within a snowpack as a function of the snow depth and the surface temperature T (Robinson et al., 2010):

$$r_f = \begin{cases} 0 & d = 0 \\ r_{\max} f(T) & 0 < d \leq 1 \\ r_{\max} + [(1 - r_{\max})(d-1)] & 1 < d \leq 2 \\ 1 & d > 2 \end{cases} \tag{22}$$

When the snow depth is below one meter the refreezing fraction is determined by the maximum fraction of refreezing $r_{\max}$ and the fraction of snow of total precipitation (Eqn. 4). Above one meter, but below two meters, the refreezing fraction increases linearly and reaches its maximum at two meters. The thickness of superimposed ice $h_{\text{s.ice}}$ is derived form the first part of Equation 21.

2.10 Calibration and evaluation

The response of the model to parameters is complex because, for example, a change of the melt component indirectly also alters the surface albedo due to feedbacks to impurity accumulation and the surface type. Due to these feedbacks we use a Monte Carlo approach to calibrate the model. As the criteria of the performance of the model we want to minimize the sum of the differences of albedo simulation and observation during the period of April 1 to September 30:

$$\sum_{01.04}^{30.09} |\alpha_s - \alpha_{\text{AWS}}| \tag{23}$$

10

where α_s is the simulated surface albedo (Eqn. 18) and α_{AWS} is the albedo derived from data of the automatic weather stations. Reference surface albedo is calculated from daily mean data from the GEUS stations and hourly data for IMAU stations, where only data with a solar zenith angle below 75° is used. The calibration covers one full ablation season after a spin-up of 100 years. The long spin-up is required to reach equilibrium with all possible parameter combinations.

We chose the free parameters based on available data. The free parameters are: the critical snow depth d_{crit}, the active fraction of BC and dust on ice $\mathcal{F}$, the reduction fraction on ice r_{ice}, the specific surface area of ice $\hat{S}$ and the albedo of clean wet snow $\alpha_{\hat{S},ws}$ without the effect of clouds, and the solar zenith angle.

The range of parameters is shown in Figure 5. The critical snow depth determines the rate of change from the summer to the winter surface albedo as well as the change from wet snow to bare ice. It cannot be measured and is therefore a free parameter. The active fraction bundles all surface processes together and is a free parameter which accounts for impurity dynamics on the ice surface and cryoconite hole formation. The runoff fraction on ice is also a free parameter, as it is currently not observed and the range of the runoff fraction is derived from observed impurity masses on the GrIS ablation zone. The specific surface area of ice needs to be calibrated because data is sparse and the parameter range is based on Dadic et al. (2013). The albedo of wet snow accounts for grain growth and is not directly measured, and therefore also calibrated.

The calibration period of one season makes it possible to calibrate and evaluate the model on the same dataset. The model is calibrated on data of one year and then applied to the remaining period. This makes it possible to investigate the variability of the free parameters.

2.11 Forcing data

Station KAN_M (1270 m a.s.l.) and S5 (460 m a.s.l.) are chosen as the test sites. S5 is situated in the lower ablation zone with high melt rates and little accumulation, and KAN_M is located in the dark area. A simulation of the impurity accumulation, the surface albedo and the SMB requires – besides the common parameters listed in Table 1 and the free parameters – the following inputs: temperature and precipitation, the atmospheric input rates (k_I, k_{II}), and the concentrations of dust and BC in ice.

The temperature parameters $T_\oplus$ and ς are fitted for each year to the observations for the calibration and over the whole period of measurements (2005-2012) for the model runs marked with "mean". Since the precipitation is not recorded by the AWS we used output of a regional climate model (MAR; Tedesco et al. (2014)) to derive $\overline{P}$.

The atmospheric input rate from distant sources (k_I) of BC is $0.001 \, \mathrm{g \, m^{-2} \, a^{-1}}$ obtained from ice cores (Lee et al., 2013). For dust the atmospheric deposition is $0.01 \, \mathrm{g \, m^{-2} \, a^{-1}}$, based on model simulation (Mahowald et al., 2011) and ice core analysis (Albani et al., 2015). The local atmospheric input (k_{II}) for both dust and BC is set to zero, since we do not distinguish between those two sources at the moment.

11

The englacial concentration ($[\iota_{\text{englacial,n}}]$) of dust and BC can be provided by a tracer transport module (Goelles et al., 2015), but in this study we will use data from ice cores Wientjes et al. (2012). The englacial concentration of BC at KAN_M is $4\,\text{ng}\,\text{g}^{-1}$, based on the core at S8 (7.25 km southwest). At S5 the BC concentration is $1\,\text{ng}\,\text{g}^{-1}$, based on the nearby S1 core.

Dust concentration measurements were not included in the shallow cores above, therefore the dust concentrations are based on the NGRIP core (Ruth, 2007). Since KAN_M is located in the dark area we assume a higher dust concentration of $2000\,\text{ng}\,\text{g}^{-1}$ and a lower one of $100\,\text{ng}\,\text{g}^{-1}$ at S5.

3 Modeling results

3.1 Calibration

Figure 5 presents an overview of simulated and measured surface albedos with the ranges and values of the free parameters listed in the lower section of the graph (surface height change can be seen Figure S5). The measured albedo in the summer of 2009 is about 0.20 higher than in the following years. If the model is calibrated on data of 2009 (orange) the match to observed data in 2010 and later is poor. Similarly, if the model is calibrated with data of 2010, 2011 or 2012 it underestimates the ice albedo in 2009.

The reduction fraction on ice r_{ice} and the wet snow albedo $\alpha_{\hat{S},\text{ws}}$ are similar for all four calibrations. In contrast, the active fraction $\mathcal{F}$ and critical snow depth d_{crit} vary over the whole range. The model realization "2010:Mean" uses the parameters from the 2010 calibration, the mean precipitation rate at the location $\overline{P}$ ($2.24\,10^{-8}\,\text{m w.e}\,\text{s}^{-1}$), and the mean temperature parameters $T_{\oplus}$ (1.39 °C with a SD of 0.04) and ς (0.23 °C day^{-1}). The resulting albedo of "2010:Mean" matches the 2010 simulation closely.

3.2 Station KAN_M in 2010

Figure 6 displays the simulations of the KAN_M station in the year 2010. The amount of dust and BC inside the snowpack (panel c) builds up until all the snow has melted in June (panel e). At the same time, superimposed ice has formed (panel f, and Figure S5) which was assumed to hold no impurities. This causes a drop in dust concentration immediately after the ice is exposed since the amount of released dust by snow melt is insignificant and the constant runoff kicks in. In contrast, the BC contribution from snow melt causes a sudden increase of the BC amount as ice is exposed, which soon afterward is reduced due to the same effect.

The lowering of the albedo from March to May is solely due the effect of the zenith angle. Similarly, the albedo variation during summer (panel g) is also due to the solar zenith angle since the variation of dust and BC (panel d) are too low to visibly alter the albedo.

The model realization "2010:Mean" uses the free parameters of the 2010 calibration, but the temperature and precipitation parameterization is derived from the mean values over the whole period

12

(2005-2012). The resulting albedo (magenta) is almost indistinguishable from the model with the parameterizations of temperature and precipitation derived from the 2010 data (green).

355 The simulated maximum amount of BC on the ice surface is $0.068\,\mathrm{g\,m^{-2}}$ and of dust is $29.55\,\mathrm{g\,m^{-2}}$. Hence, the mass of dust on the ice surface is 434 times larger than BC. The maximum amount in the snowpack is $0.75\,\mathrm{mg\,m^{-2}}$ BC and $7.45\,\mathrm{mg\,m^{-2}}$ dust.

3.3 Stations S5 in 2011

Figure 7 displays the simulation of station S5 in 2011 with the parameters shown in Figure 5. The
360 duration of the snow cover is more than a month shorter (panel e) when the temperature and precipitation parameterization is used. This is caused by the overestimated temperature in May (panel a).

The simulated impurity concentrations are lower than at KAN_M due to the lower concentrations of englacial BC and dust. Where the maximum amount of BC on the ice surface is $0.06\,\mathrm{g\,m^{-2}}$ and
365 of dust is $4.04\,\mathrm{g\,m^{-2}}$, which is about 67 times more than BC. Therefore, the albedo lowering at S5 is mostly caused by BC due to the 200 times higher absorption. The maximum amount in the snowpack is also lower than at KAN_M, due to the shorter duration of snow cover ($0.638\,\mathrm{mg\,m^{-2}}$ BC and $6.383\,\mathrm{mg\,m^{-2}}$ dust).

The measured SMB at S5 in 2011 was -4.06 meters, while the simulation yielded -2.98 meters.
370 This is mainly due to the overestimated albedo combined with a too-low transmissivity until May, causing a too-low net shortwave radiation (see Figure S6 in the supplements). A graph similar to Figure 5 for station S5 can be found in the supplements (Figure S7).

4 Discussion

4.1 Assumptions and uncertainties

375 Due to the design goal, we chose a simplified energy balance, a single-layer snowpack model and a parameterization of near-surface temperature and precipitation. Therefore, it has to be clear that the model can not compete with full energy balance studies performed in the same area. The goal was that the model takes impurity accumulation into account and that it can be used as an alternative to positive degree day models, with only a few required inputs. The simplified energy balance is
380 largely based on Robinson et al. (2010) (sections 2.3, 2.7, 2.8, 2.9) where the associated uncertainties have been studied in detail in Fitzgerald et al. (2012). We now briefly discuss the assumptions and uncertainties of each model component, again in the order of the flow chart (Fig. 2).

The temperature parameterization follows the observation reasonably well during the melt period. Also the low standard deviations of $T_{\oplus}$ at both stations is an indicator of the quality of the temper-
385 ature parameterization. At station S5 the start of the positive temperatures was set too early in the presented year and others, causing a too-early melt initiation of the seasonal snow. Further analysis

13

of AWS data is needed in order to derive a parameterization of the start and end dates of positive temperatures which is valid for the whole GrIS.

The precipitation parameterization via the annual mean yields similar snow-depth evolution as when the daily precipitation data from the MAR model is used. Our parameterization neglects summer snowfall and makes it impossible to account for snow grain growth, which has a big influence on the albedo of snow. Nevertheless, for its simplicity, the precipitation parameterization performs sufficiently well.

The next component to discuss is the impurity accumulation inside the snowpack and on the ice surface. The impurity accumulation inside the snowpack depends solely on the atmospheric inputs and biological production. Since the atmospheric fallout rates of both BC and dust are low, the impact on the albedo of snow is also low (see Fig. S2). The constant influx of dust and BC is a simplification – in nature the influx of impurities is very erratic – as can be seen in ice core records (Ruth, 2007; McConnell et al., 2007). Therefore, the increase of impurity concentration inside the snowpack also follows this erratic behavior in nature. A time-depended influx of dust and BC could be obtained from atmospheric models in the future which would allow a more detailed study of the accumulation zone. Along with a multilayer snowpack model and a more sophisticated snow albedo model which takes aging and impurities into account.

In addition to the atmospheric input, the impurity accumulation on the ice surface depends on ice melt and the englacial concentration via the source k_{III} and the reduction term. The englacial value of BC was obtained from nearby located shallow ice cores. Englacial values of impurities can differ substantially over a short distance due the erratic nature of impurity deposition. Short ice cores located at the AWS sites as well as measurements of surface impurities would be needed to further study the effect of the impurity melt-out. In addition, time-lapse cameras on the weather masts and frequent measurements of surface concentrations could be used to derive the reduction term.

Model snow albedo was unaffected by impurities and only indirectly affected by grain growth. The effect of impurities in snow at the ablation zone is short and low (see also Fig. S2), but the grain growth could cause a difference in surface albedo of more than 0.20. In general, the fixed dry snow albedo matches the observations well until the onset of melt. During snow melt the match becomes weaker due to the neglected grain growth. A time-dependent parameterization which gradually lowers the albedo of snow after the onset of melt might improve the albedo match in spring. Although the period of snow cover can be long, the effects of the snow albedo on melt in the ablation zone is limited due to the low incoming radiation when the seasonal snow cover is still intact. Nevertheless, in the accumulation zone the snow albedo has a big impact on the overall SMB of the GrIS due to the huge area.

The biggest uncertainties connected with the ice albedo are the active fraction and the parameterization of the albedo reduction due to impurities. The parameterization of ice albedo (Eqn. 10) assumes externally mixture of carbon particles (located outside of ice grains) (Gardner and Sharp,

2010). We assumed that particles located on the ice surface have a similar effect on impurities as this external mixture. This might be an oversimplification which most likely will not hold at very high concentrations when the radiation is fully absorbed at the surface by the particles. A study of impurities located *on* the ice surface is required in order to further test this assumption or replace the parameterization by one which takes surface concentrations into account.

The active fraction varies over the whole range, in Figure 5. This is partly due to model ambiguity: many parameter combinations can lead to the same result. So could a high specific surface area combined with a high active fraction lead to the same result as a low specific surface area and a lower active fraction. Therefore, better constrains on the specific surface area are required in order to lower the uncertainty of the active fraction. Similarly, a high impurity concentration and a low active fraction can have the same effect as a low concentration and a high active fraction. Therefore, direct measurements on the englacial concentration as well as observations of dust and BC deposition can further constrain the active fraction. The active fraction itself could possibly be obtained by time-lapse cameras and further studies on the dynamics of cryoconite holes.

The lower albedos at KAN_M after 2009 could have been caused by an increase in the active fraction – for example, by the releases of impurities from cryoconite holes. Since dynamics of the active fraction, i.e. the surface processes, are not captured at the moment, no model setup is able to capture 2009 and 2010. For now, the active fraction bundles all surface processes together, but it could be a model component on its own in the future.

Both the albedo of snow and ice are altered by clouds. We developed a linear parameterization of clouds by elevation which introduces a mean error of about $\pm$ 0.02 (see Figure S1a). Since this linear parameterization gives a constant albedo alteration due to clouds, the albedo is overestimated by up to 0.10 on days with a clear sky.

The zenith angle of the sun has a high impact on the albedo of ice due to its low specific surface area. Since the angle of the sun is easy to derive accurately the associated uncertainties are low and solely determined by the parameterization. Also, the slope of the GrIS is small and therefore plays no role in the effective zenith angle, while this might not be the case for steep valley glaciers.

The free parameter of the surface albedo component (Eqn. 18) is the critical snow depth which ranges from 0.01 to 0.20 m w.e.. The change of the measured albedo in the autumn of the years 2010, 2011 and 2012 at KAN_M is abrupt after the first snowfall, which is reflected in a low critical snow depth at those years. The highest critical snow depth was calibrated at S5, where ice might be exposed the whole time due to low accumulation rate and wind drift. Therefore, S5 is not suited to calibrate the critical snow-depth. Hence, the critical snow depth is in the region of 0.02 m w.e..

The potential melt rate influences the surface albedo indirectly via feedbacks to impurity melt-out and via the snow depth. Most significantly it determines the SMB which could be used as a boundary condition for glacier and ice sheet models. Potential melt was calculated with a simplified energy balance which depends on, in addition to the surface albedo, two empirical parameters: the inso-

lation on top of the atmosphere and the transmissivity. The transmissivity used in previous studies (Robinson et al., 2010, 2011) was found to be too low. In this study we derived it by comparison of modeled and observed net shortwave radiation. Therefore, the overall effect of transmissivity is captured well (see Figure S4 in the supplements). Nevertheless, similar to the effect of clouds on albedo, the melt rate is underestimated on clear sky days because the transmissivity was assumed to be constant.

Overall, the performance of the model is satisfying, especially of the net radiation (see Fig. S4 and S6), even though the parameterization of temperature and precipitation is very simple. The model calibration of 2010 at KAN_M with mean temperature and precipitation parameters performs well both at KAN_M and S5, an therefore represents the best parameter set.

4.2 Melt-out and runoff of impurities

Dust is the main contributor to impurity mass at both stations, which was also found in observations at different places of the GrIS (Bøggild et al., 2010; Takeuchi et al., 2014). The question is which is the main source of dust and BC on ice: melt-out or the atmospheric sources? The accumulated impurity mass at KAN_M is about ten times larger than at S5. This indicates that melt-out is the main contributor to impurity mass since the atmospheric input rates are the same for both station and the similar impurity runoff (r_{ice} see Figure 5).

One meter of ice melt releases englacial impurities, which have been deposited over years or decades in the accumulation zone several thousand years ago. Dust concentrations during the last glacial are 10-100 times higher than during the Holocene (Steffensen, 1997). Therefore, currently dust melt-out dominates over atmospheric deposition. For example, one meter melt of ice with a dust concentration of $1,000\,\mathrm{ng\,g^{-1}}$ releases $0.91\,\mathrm{g\,m^{-2}}$ of dust. At the current rate of atmospheric deposition from large-scale transport it would take about 100 years to deposit the same amount of dust (see also Figure S8).

Atmospheric deposition of dust could play a significant role close to the margin if the transport by wind from the surrounding tundra is effective. The local dust source is likely restricted to the outermost ablation zone because of the prevailing katabatic winds. Therefore, there might be a "threshold elevation" up to which local dust from the tundra contributes significantly. Above this threshold, large-scale transport from other continents dominates.

For BC the answer is less clear. Ice formed during 1851 to 1951 has a mean concentration of BC of $4\,\mathrm{ng\,g^{-1}}$, while the pre-industrial concentration is $1.7\,\mathrm{ng\,g^{-1}}$ (McConnell et al., 2007). Atmospheric deposition is the dominant source of BC, up to annual melt rates of one meter and a BC concentrations of $1.0\,\mathrm{ng\,g^{-1}}$ (see Figure S8). At higher melt rates melt-out dominates, but the atmospheric deposition still contributes significantly to the amount of BC on the ice surface.

The reduction fraction r_{ice} of 0.001 per day causes a residence time of the impurities on the ice surface of several decades. This is linked to the slow movement of cryoconite on an exposed ice

16

surface, as has been measured on Longyearbreen, Svalbard (Irvine-Fynn et al., 2011). It takes more than 56 years in order to reduce from 30 $\mathrm{g\,m^{-2}}$ to below one $\mathrm{g\,m^{-2}}$ by assuming 60 days with exposed ice and exponential decay with one permille per day. Therefore, the impurities enhance ice melt over decades after deposition by melt-out or via the atmosphere.

5 Conclusions

We developed a surface mass balance model which includes the effect of accumulation of dust and black carbon on the albedo of ice, besides the effects of clouds and the zenith angle of the sun. The model requires only a small number of inputs and is therefore suitable as the surface mass balance component of standalone ice sheet or glacier models.

The inferred runoff of impurities is in the order of one permille per day, which corresponds to a residence time of decades on the ice surface during which the albedo is lowered and melt is enhanced. Dust is the main contributor to impurity mass, of which melt-out is the main source. Melt-out of BC is the dominant source at annual melt rates above one meter. Current atmospheric deposition of BC contributes considerably to the total amount of BC on the ice surface. Therefore, mitigation of BC emissions has an immediate effect on the albedo of the ice surface.

The system has a positive feedback between impurity melt-out and ice melt due to the decadal residence time and the dominant source of melt-out. A high melt event releases large amounts of englacial impurities from within the ice, which lower the albedo and in turn enhances melt. Which then feeds back and causes more impurities to melt-out.

The presented model can be used to study the long-term effect of dust and BC on the future melt of the GrIS and smaller glaciers. Goelles et al. (2015) applied the model to a simplified geometry mimicking the GrIS. They found that, without considering all feedback processes, an additional mass loss of up to 7 percent in the year 3000 can be expected if impurity melt-out and accumulation is considered.

The Supplement related to this article is available online at doi:10.5194/tc-0-1-2016-supplement.

References

Albani, S., Mahowald, N. M., Winckler, G., Anderson, R. F., Bradtmiller, L. I., Delmonte, B., François, R., Goman, M., Heavens, N. G., Hesse, P. P., Hovan, S. A., Kang, S. G., Kohfeld, K. E., Lu, H., Maggi, V., Mason, J. A., Mayewski, P. A., McGee, D., Miao, X., Otto-Bliesner, B. L., Perry, A. T., Pourmand, A., Roberts, H. M., Rosenbloom, N., Stevens, T., and Sun, J.: Twelve thousand years of dust: the Holocene global dust cycle constrained by natural archives, Climate of the Past, 11, 869–903, doi:10.5194/cp-11-869-2015, 2015.

Bales, R. C., Guo, Q., Shen, D., McConnell, J. R., Du, G., Burkhart, J. F., Spikes, V. B., Hanna, E., and Cappelen, J.: Annual accumulation for Greenland updated using ice core data developed during 2000–2006 and analysis of daily coastal meteorological data, Journal of Geophysical Research, 114, D06 116, doi:10.1029/2008JD011208, 2009.

Bøggild, C. E., Winther, J.-G., Sand, K., and Elvehøy, H.: Sub-surface melting in blue-ice fields in Dronning Maud Land, Antarctica: observations and modelling, Annals of Glaciology, 21, 162–168, 1995.

Bøggild, C. E., Oerter, H., and Tukiainen, T.: Increased ablation of Wisconsin ice in eastern north Greenland: observations and modelling, Annals of Glaciology, 23, 144–148, 1996.

Bøggild, C. E., Brandt, R. E., Brown, K. J., and Warren, S. G.: The ablation zone in northeast Greenland: ice types, albedos and impurities, Journal of Glaciology, 56, 101–113, doi:10.3189/002214310791190776, 2010.

Bougamont, M., Bamber, J. L., and Greuell, W.: A surface mass balance model for the Greenland Ice Sheet, Journal of Geophysical Research, 110, F04 018, doi:10.1029/2005JF000348, 2005.

Brutel-Vuilmet, C., Menegoz, M., and Krinner, G.: An analysis of present and future seasonal Northern Hemisphere land snow cover simulated by CMIP5 coupled climate models, The Cryosphere, 7, 67–80, doi:10.5194/tc-7-67-2013, 2013.

Burgess, E. W., Forster, R. R., Box, J. E., Mosley-Thompson, E., Bromwich, D. H., Bales, R. C., and Smith, L. C.: A spatially calibrated model of annual accumulation rate on the Greenland Ice Sheet (1958–2007), Journal of Geophysical Research, 115, F02 004, doi:10.1029/2009JF001293, 2010.

Calanca, P., Gilgen, H., Ekholm, S., and Ohmura, A.: Gridded temperature and accumulation distributions for Greenland for use in cryospheric models, Annals of Glaciology, 31, 118–120, doi:10.3189/172756400781820345, 2000.

Chandler, D. M., Alcock, J. D., Wadham, J. L., Mackie, S. L., and Telling, J.: Seasonal changes of ice surface characteristics and productivity in the ablation zone of the Greenland Ice Sheet, The Cryosphere, 9, 487–504, doi:10.5194/tc-9-487-2015, 2015.

Dadic, R., Mullen, P. C., Schneebeli, M., Brandt, R. E., and Warren, S. G.: Effects of bubbles, cracks, and volcanic tephra on the spectral albedo of bare ice near the Transantarctic Mountains: Implications for sea glaciers on Snowball Earth, Journal of Geophysical Research-Earth Surface, 118, 1658–1676, doi:10.1002/jgrf.20098, 2013.

Dang, C., Brandt, R. E., and Warren, S. G.: Parameterizations for narrowband and broadband albedo of pure snow and snow containing mineral dust and black carbon, Journal of Geophysical Research: Atmospheres, 120, 5446–5468, doi:10.1002/2014JD022646, 2015.

Doherty, S. J., Warren, S. G., Grenfell, T. C., Clarke, A. D., and Brandt, R. E.: Light-absorbing impurities in Arctic snow, Atmospheric Chemistry and Physics, 10, 11 647–11 680, doi:10.5194/acp-10-11647-2010, 2010.

Doherty, S. J., Grenfell, T. C., Forsström, S., Hegg, D. L., Brandt, R. E., and Warren, S. G.: Observed vertical redistribution of black carbon and other insoluble light-absorbing particles in melting snow, Journal of Geophysical Research: Atmospheres, 118, 5553–5569, doi:10.1002/jgrd.50235, 2013.

Dumont, M., Brun, E., Picard, G., Michou, M., Libois, Q., Petit, J. R., Geyer, M., Morin, S., and Josse, B.: Contribution of light-absorbing impurities in snow to Greenland's darkening since 2009, Nature Geoscience, 7, 509–512, doi:10.1038/ngeo2180, 2014.

Enderlin, E. M., Howat, I. M., Jeong, S., Noh, M. J., Angelen, J. H., and Van den Broeke, M. R.: An improved mass budget for the Greenland ice sheet, Geophysical Research Letters, 41, 866–872, doi:10.1002/2013GL059010, 2014.

Fitzgerald, P. W., Bamber, J. L., Ridley, J. K., and Rougier, J. C.: Exploration of parametric uncertainty in a surface mass balance model applied to the Greenland ice sheet, Journal of Geophysical Research-Earth Surface, 117, F01 021, doi:10.1029/2011JF002067, 2012.

Gardner, A. and Sharp, M.: A review of snow and ice albedo and the development of a new physically based broadband albedo parameterization, Journal of Geophysical Research, 115, F01 009, doi:10.1029/2009JF001444, 2010.

Gent, P. R., Danabasoglu, G., Donner, L. J., Holland, M. M., Hunke, E. C., Jayne, S. R., Lawrence, D. M., Neale, R. B., Rasch, P. J., Vertenstein, M., Worley, P. H., Yang, Z.-L., and Zhang, M.: The Community Climate System Model Version 4, Journal of Climate, 24, 4973–4991, doi:10.1175/2011JCLI4083.1, 2011.

Goelles, T., Bøggild, C. E., and Greve, R.: Ice sheet mass loss caused by dust and black carbon accumulation, The Cryosphere, 9, 1845–1856, doi:10.5194/tc-9-1845-2015, 2015.

Irvine-Fynn, T. D. L., Bridge, J. W., and Hodson, A. J.: In situ quantification of supraglacial cryoconite morphodynamics using time-lapse imaging: an example from Svalbard, Journal of Glaciology, 57, 651–657, doi:10.3189/002214311797409695, 2011.

Klok, E. J. and Oerlemans, J.: Model study of the spatial distribution of the energy and mass balance of Morteratschgletscher, Switzerland, Journal of Glaciology, 48, 505–518, doi:10.3189/172756502781831133, 2002.

Lee, Y. H., Lamarque, J. F., Flanner, M. G., Jiao, C., Shindell, D. T., Berntsen, T., Bisiaux, M. M., Cao, J., Collins, W. J., Curran, M., Edwards, R., Faluvegi, G., Ghan, S., Horowitz, L. W., McConnell, J. R., Ming, J., Myhre, G., Nagashima, T., Naik, V., Rumbold, S. T., Skeie, R. B., Sudo, K., Takemura, T., Thevenon, F., Xu, B., and Yoon, J. H.: Evaluation of preindustrial to present-day black carbon and its albedo forcing from Atmospheric Chemistry and Climate Model Intercomparison Project (ACCMIP), Atmospheric Chemistry and Physics, 13, 2607–2634, doi:10.5194/acp-13-2607-2013, 2013.

Liou, K. N.: An Introduction to Atmospheric Radiation, Volume 84, Second Edition (International Geophysics), Academic Press, San Diego and London, 2 edn., 2002.

Lipscomb, W. H., Fyke, J. G., Vizcaino, M., Sacks, W. J., Wolfe, J., Vertenstein, M., Craig, A., Kluzek, E., and Lawrence, D. M.: Implementation and Initial Evaluation of the Glimmer Community Ice Sheet Model in the Community Earth System Model, Journal of Climate, 26, 7352–7371, doi:10.1175/JCLI-D-12-00557.1, 2013.

Mahowald, N. M., Albani, S., Engelstaedter, S., Winckler, G., and Goman, M.: Model insight into glacial-interglacial paleodust records, Quaternary Science Reviews, 30, 832–854, doi:10.1016/j.quascirev.2010.09.007, 2011.

McConnell, J., Edwards, R., Kok, G., Flanner, M., Zender, C. S., Saltzman, E., Banta, J., Pasteris, D., Carter, M., and Kahl, J.: 20th-century industrial black carbon emissions altered arctic climate forcing, Science, 317, 1381–1384, doi:10.1126/science.1144856, 2007.

Mernild, S. H., Liston, G. E., Hiemstra, C. A., and Christensen, J. H.: Greenland Ice Sheet Surface Mass-Balance Modeling in a 131-Yr Perspective, 1950–2080, Journal of Hydrometeorology, 11, 3–25, doi:10.1175/2009JHM1140.1, 2010.

Moustafa, S. E., Rennermalm, A. K., Smith, L. C., Miller, M. A., Mioduszewski, J. R., Koenig, L. S., Hom, M. G., and Shuman, C. A.: Multi-modal albedo distributions in the ablation area of the southwestern Greenland Ice Sheet, The Cryosphere, 9, 905–923, doi:10.5194/tc-9-905-2015, 2015.

Noël, B., Van de Berg, W. J., van Meijgaard, E., Kuipers Munneke, P., Van de Wal, R. S. W., and Van den Broeke, M. R.: Evaluation of the updated regional climate model RACMO2.3 : Summer snowfall impact on the Greenland Ice Sheet, The Cryosphere, 9, 1831–1844, doi:10.5194/tc-9-1831-2015, 2015.

Oaida, C. M., Xue, Y., Flanner, M. G., Skiles, S. M., De Sales, F., and Painter, T. H.: Improving snow albedo processes in WRF/SSiB regional climate model to assess impact of dust and black carbon in snow on surface energy balance and hydrology over western U.S., Journal of Geophysical Research: Atmospheres, 120, 3228–3248, doi:10.1002/2014JD022444, 2015.

Oerlemans, J.: A model for the surface balance of ice masses: Part I: alpine glaciers, Zeitschrift für Gletscherkunde und Glacialgeologie, 27, 63–83, 1991.

Oerlemans, J.: Glaciers and climate change, A.A. Balkema Publishers, Lisse, Abingdon, Exton (PA), Tokyo, 2001.

Oerlemans, J., Giesen, R. H., and Van den Broeke, M. R.: Retreating alpine glaciers: increased melt rates due to accumulation of dust (Vadret da Morteratsch, Switzerland), Journal of Glaciology, 55, 729–736, doi:10.3189/002214309789470969, 2009.

Rae, J. G. L., Aðalgeirsdóttir, G., Edwards, T. L., Fettweis, X., Gregory, J. M., Hewitt, H. T., Lowe, J. A., Lucas-Picher, b. P., Mottram, R. H., Payne, A. J., Ridley, J. K., Shannon, S. R., Van de Berg, W. J., Van de Wal, R. S. W., and Van den Broeke, M. R.: Greenland ice sheet surface mass balance: evaluating simulations and making projections with regional climate models, The Cryosphere, 6, 1275–1294, doi:10.5194/tc-6-1275-2012, 2012.

Reeh, N.: Parameterization of Melt Rate and Surfaee Temperature on the Greenland lee Sheet, Polarforschung, 53, 113–128, 1991.

Reeh, N., Oerter, H., Letréguilly, A., Miller, H., and Hubberten, H.-W.: A new, detailed ice-age oxygen-18 record from the ice-sheet margin in central West Greenland, Palaeogeography, Palaeoclimatology, Palaeoecology (Global and Planetary Change Section), 4, 373–383, doi:10.1016/0921-8181(91)90003-F, 1991.

Remias, D., Holzinger, A., Aigner, S., and Luetz, C.: Ecophysiology and ultrastructure of Ancylonema nordenskioldii (Zygnematales, Streptophyta), causing brown ice on glaciers in Svalbard (high arctic), Polar Biology, 35, 899–908, doi:10.1007/s00300-011-1135-6, 2012.

Robinson, A., Calov, R., and Ganopolski, A.: An efficient regional energy-moisture balance model for simulation of the Greenland Ice Sheet response to climate change, The Cryosphere, 4, 129–144, doi:10.5194/tc-4-129-2010, 2010.

Robinson, A., Calov, R., and Ganopolski, A.: Greenland ice sheet model parameters constrained using simulations of the Eemian Interglacial, Climate of the Past, 7, 381–396, doi:10.5194/cp-7-381-2011, 2011.

Ruth, U.: Dust concentration in the NGRIP ice core, doi:10.1594/PANGAEA.587836, Supplement to: Ruth, U., Bigler, M., Röthlisberger, R., Siggaard-Andersen, M.-L., Kipf- stuhl, J., Goto-Azuma, K., Hansson, M. E., Johnsen, S. J., Lu, H., and Steffensen, J. P.: Ice core evidence for a very tight link between North Atlantic and east Asian glacial climate, Geophysical Research Letters, 34, L03 706, doi:10.1029/2006GL027876, 2007.

Ruth, U., Wagenbach, D., Steffensen, J. P., and Bigler, M.: Continuous record of microparticle concentration and size distribution in the central Greenland NGRIP ice core during the last glacial period, Journal of Geophysical Research, 108, 4098, doi:10.1029/2002JD002376, 2003.

Steffensen, J. P.: The size distribution of microparticles from selected segments of the Greenland Ice Core Project ice core representing different climatic periods, Journal of Geophysical Research, 102, 26 755–26 763, doi:10.1029/97JC01490, 1997.

Stibal, M., Šabacká, M., and Žárský, J.: Biological processes on glacier and ice sheet surfaces, Nature Geoscience, 5, 771–774, doi:10.1038/ngeo1611, 2012.

Takeuchi, N.: Optical characteristics of cryoconite (surface dust) on glaciers: the relationship between light absorbency and the property of organic matter contained in the cryoconite, Annals of Glaciology, 34, 409–414, doi:10.3189/172756402781817743, 2002.

Takeuchi, N., Kohshima, S., and Seko, K.: Structure, formation, and darkening process of albedo-reducing material (cryoconite) on a Himalayan glacier: A granular algal mat growing on the glacier, Arctic Antarctic and Alpine Research, 33, 115–122, doi:10.2307/1552211, 2001.

Takeuchi, N., Nagatsuka, N., Uetake, J., and Shimada, R.: Spatial variations in impurities (cryoconite) on glaciers in northwest Greenland, Bulletin of Glaciological Research, 32, 85–94, doi:10.5331/bgr.32.85, 2014.

Tedesco, M., Fettweis, X., Van den Broeke, M. R., Van de Wal, R. S. W., Smeets, C. J. P. P., Van de Berg, W. J., Serreze, M. C., and Box, J. E.: The role of albedo and accumulation in the 2010 melting record in Greenland, Environmental Research Letters, 6, 014 005, doi:10.1088/1748-9326/6/1/014005, 2011.

Tedesco, M., Fettweis, X., Alexander, P., Green, G., and Datta, T.: MAR Greenland Outputs from Outputs 2005-01-01 to 2013-01-01 ver. 3.2, CCNY Digital Archive, 2014.

van Angelen, J. H., Lenaerts, J. T. M., Lhermitte, S., Fettweis, X., Kuipers Munneke, P., Van den Broeke, M. R., van Meijgaard, E., and Smeets, C. J. P. P.: Sensitivity of Greenland Ice Sheet surface mass balance to surface albedo parameterization: a study with a regional climate model, The Cryosphere, 6, 1175–1186, doi:10.5194/tc-6-1175-2012, 2012.

Van den Berg, J., Van de Wal, R. S. W., and Oerlemans, J.: A mass balance model for the Eurasian ice sheet for the last 120,000 years, Global and Planetary Change, 61, 194–208, doi:10.1016/j.gloplacha.2007.08.015, 2008.

Van den Broeke, M. R., Smeets, P., Ettema, J., and Munneke, P. K.: Surface radiation balance in the ablation zone of the west Greenland ice sheet, Journal of Geophysical Research: Atmospheres, 113, D13 105, doi:10.1029/2007JD009283, 2008.

Vizcaino, M., Lipscomb, W. H., Sacks, W. J., and Van den Broeke, M. R.: Greenland Surface Mass Balance as Simulated by the Community Earth System Model. Part II: Twenty-First-Century Changes, Journal of Climate, 27, 215–226, doi:10.1175/JCLI-D-12-00588.1, 2014.

Warren, S. G. and Brandt, R. E.: Optical constants of ice from the ultraviolet to the microwave: A revised compilation, Journal of Geophysical Research, 113, D14 220, doi:10.1029/2007JD009744, 2008.

Warren, S. G. and Wiscombe, W. J.: A model for the spectral albedo of snow. II: Snow containing atmospheric aerosols, Journal Of The Atmospheric Sciences, 37, 2734–2745, 1980.

Wientjes, I. G. M. and Oerlemans, J.: An explanation for the dark region in the western melt zone of the Greenland ice sheet, The Cryosphere, 4, 261–268, doi:10.5194/tc-4-261-2010, 2010.

Wientjes, I. G. M., Van de Wal, R. S. W., Reichart, G. J., Sluijs, A., and Oerlemans, J.: Dust from the dark region in the western ablation zone of the Greenland ice sheet, The Cryosphere, 5, 589–601, doi:10.5194/tc-5-589-2011, 2011.

Wientjes, I. G. M., Van de Wal, R. S. W., Schwikowski, M., Zapf, A., Fahrni, S., and Wacker, L.: Carbonaceous particles reveal that Late Holocene dust causes the dark region in the western ablation zone of the Greenland ice sheet, Journal of Glaciology, 58, 787–794, doi:10.3189/2012JoG11J165, 2012.

Wiscombe, W. J. and Warren, S. G.: A model for the spectral albedo of snow. I: Pure snow, Journal Of The Atmospheric Sciences, 37, 2712–2733, 1980.

Wolfram Research, Inc.: Mathematica, Champaign, Illinois, 2014.

Yallop, M. L., Anesio, A. M., Perkins, R. G., Cook, J., Telling, J., Fagan, D., MacFarlane, J., Stibal, M., Barker, G., Bellas, C., Hodson, A., Tranter, M., Wadham, J., and Roberts, N. W.: Photophysiology and albedo-changing potential of the ice algal community on the surface of the Greenland ice sheet, Isme Journal, 6, 2302–2313, doi:10.1038/ismej.2012.107, 2012.

Zuo, Z. and Oerlemans, J.: Modelling albedo and specific balance of the Greenland ice sheet: Calculations for the Sondre Stromfjord transect, Journal of Glaciology, 42, 305–317, 1996.

23

Table 1. Standard physical parameters.

Symbol	Constant	Value	Unit
ρ_{ice}	Density of ice	910	kg m^{-3}
ρ_{w}	Density of water	1000	kg m^{-3}
$t_{\odot,\text{start}}$	Start of summer	121	day of the year
$t_{\odot,\text{end}}$	End of summer	244	day of the year
λ	Long-wave radiation coefficient	10	$\text{W m}^{-2}\,\text{K}^{-1}$
c	Melt model coefficient	-55	W m^{-2}
r_{max}	Maximum fraction of refreezing	0.6	–
L_{m}	Latent heat for melting of ice	334 000	J kg
d_{eff}	Effective depth on ice	5	m
$\alpha_{\hat{S},ds}$	Dry snow albedo, zenith angle 0, no clouds	0.65	
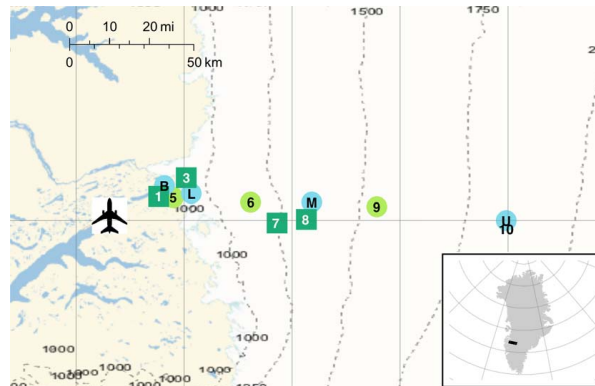
Figure 1. Weather stations and sampling sites at the K-transect in western Greenland, near the Kangerlussuaq airport. Blue circles mark the PROMICE weather stations operated by GEUS (without their prefix "KAN_") and the green circles mark the ones operated by IMAU (without their prefix "S"). The squares mark additional mass balance sites where ice samples have been taken (Wientjes et al., 2012). Station S9 is located near the equilibrium line and sites S6, S7, S8 and KAN_M are located in the "dark region" with lower albedos.

24
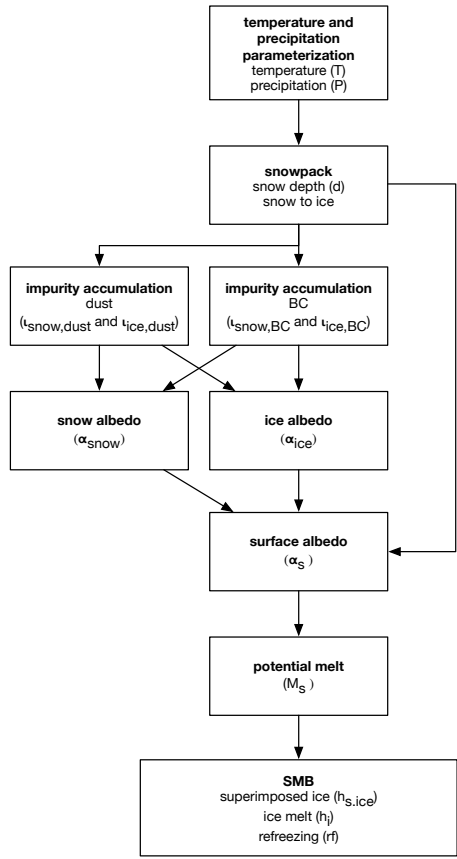
Figure 2. Flow chart of the surface albedo and surface mass balance model for one time-step of one day.
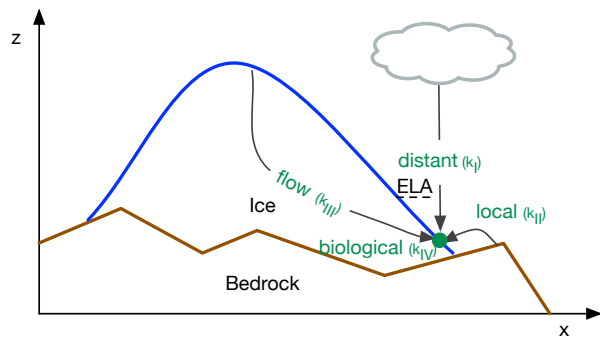
Figure 3. Cross section through an ice sheet and four different sources of impurities in the ablation zone. ELA stands for equilibrium line altitude.
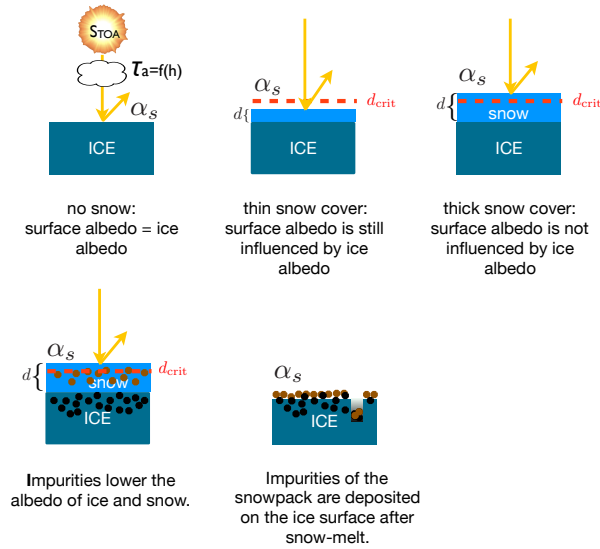
Figure 4. The relationship between ice albedo, snow albedo and impurity concentration to surface albedo α_s. The surface albedo is still influenced by the underlaying ice surface if the snow depth (d) is lower than the critical snow depth d_{crit}.
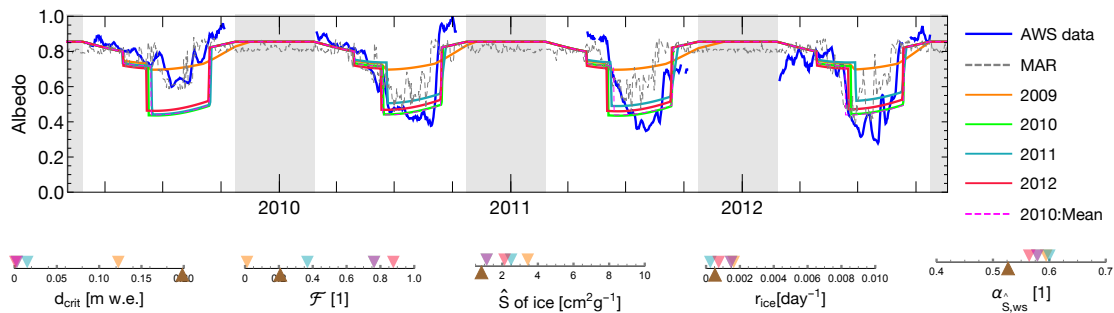
Figure 5. Albedo evolution of the KAN_M station from 2009 to 2012. The lower section of the graph presents the free parameter realizations. Each year has its own color code in the albedo chart and the parameter overview. In addition, the parameter set of S5 in 2011 is shown in brown below the scale. The albedo data of the AWS (in blue) and of the regional climate model MAR (in dashed black) are shown for comparison and are smoothed with a moving average over a seven-day window. Grey areas indicate periods when the sun zenith angle is higher than $90°$ (i.e. the sun is below the horizon at mid-day).

26
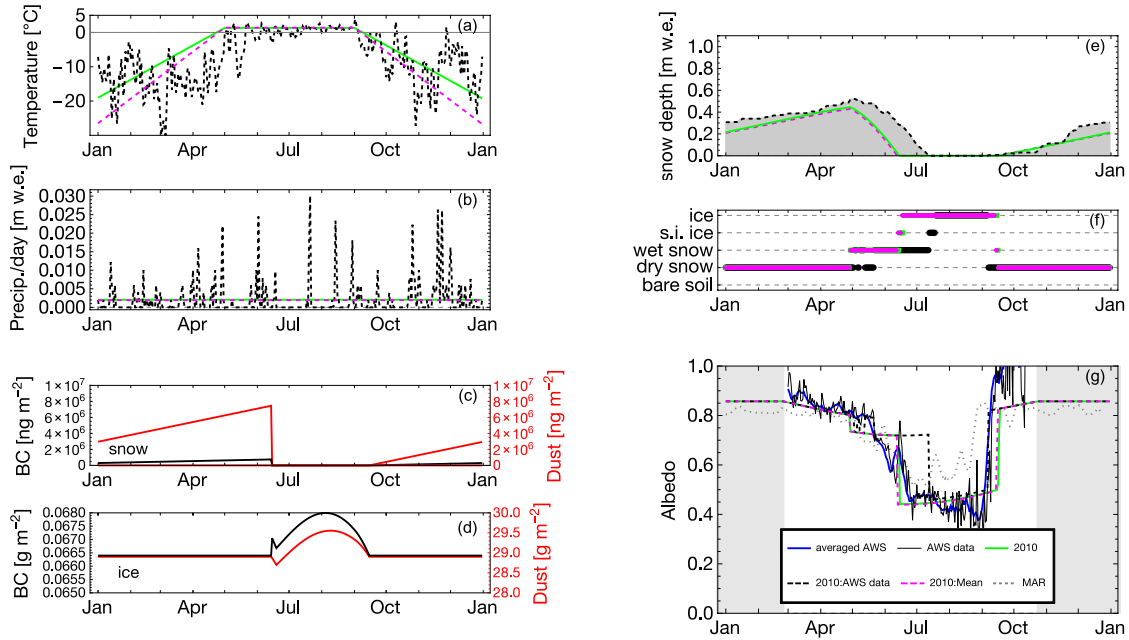
Figure 6. Detailed result of station KAN_M in 2010. **(a)** near-surface temperature parameterization in green, observation in dashed black and the mean (2005-2012) in magenta. **(b)** daily precipitation from regional climate model MAR (dashed black), the parameterization in green, and the mean parameterization in magenta. **(c, d)** shows the evolution of dust (red) and BC (black) inside the snowpack and on the ice surface. **(e)** snow depth evolution with the parameterized temperature and precipitation in green, the "2010:Mean" model in magenta and the model with temperature from the AWS station and precipitation from the MAR model in black. **(f)** surface type; s.i. ice stands for superimposed ice. **(g)** surface albedo evolution of the smoothed (over 7 days, in blue) and the original AWS data (thin black line). The simulation "2010:AWS data" uses the actual AWS temperature and MAR precipitation, and simulation "2010:Mean" the temperature and precipitation means.
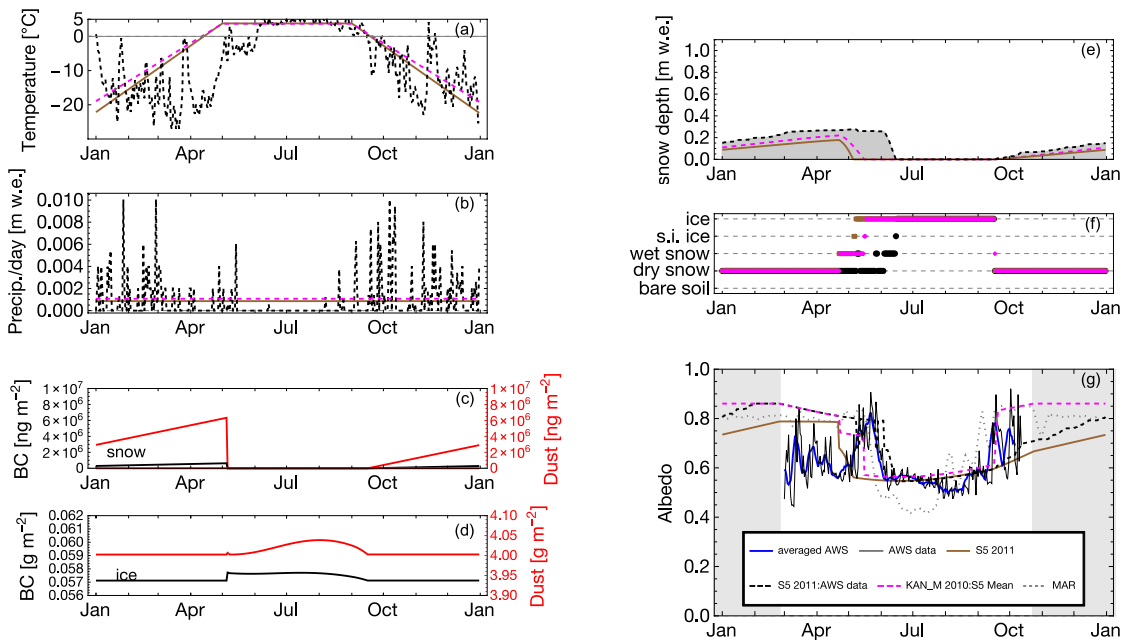
Figure 7. Details of station S5 in the year 2011 with the same plot arrangement as in Fig. 6. The model realization "KAN_M 2010: S5 Mean" uses the same parameters as the KAN_M 2010 configuration, but with the S5 mean values of temperature and precipitation or $\overline{P}$ (1.24 10^{-8} m w.e s^{-1}) , $T_\oplus$ (3.70°C with a SD of 0.02) and ς (0.19 °C day^{-1})
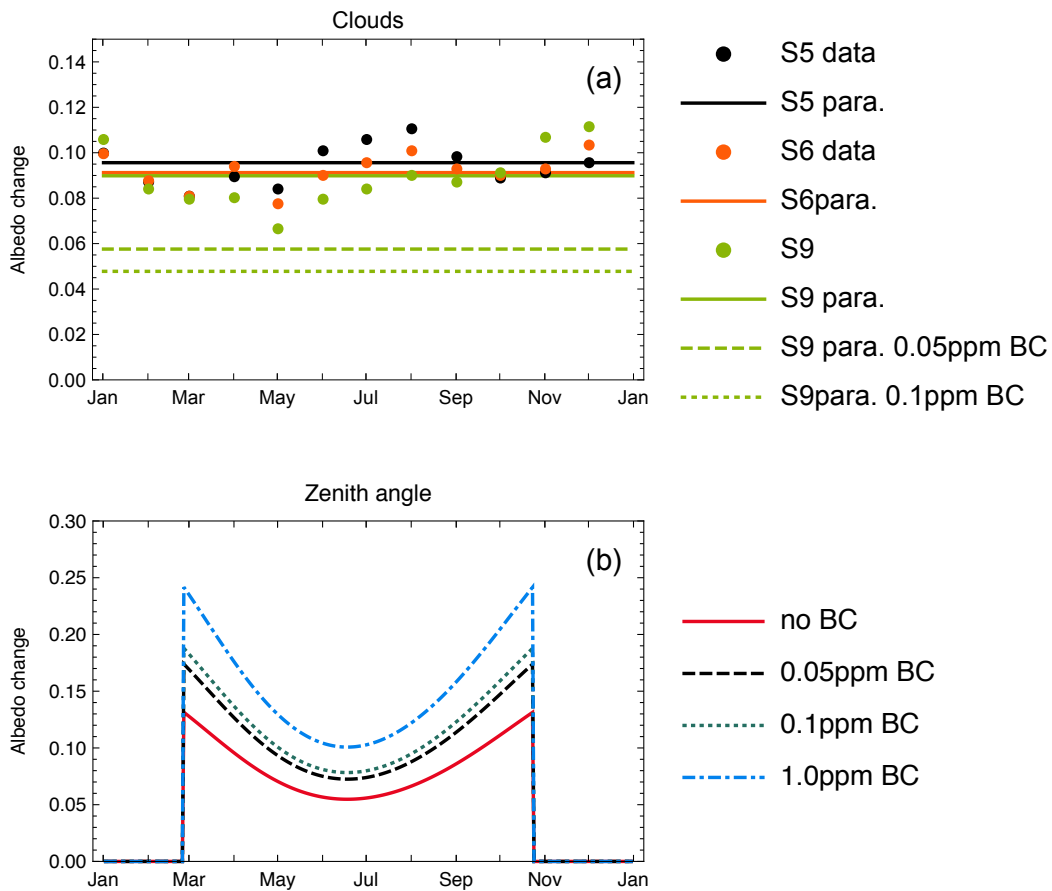
FIGURE S1. Albedo effect of clouds (a) and the zenith angle of the sun (b) at the K-transect. Calculated by Equations 14 and 16, based on a specific surface area of ice of 2 cm^{2}g^{-1}. The dots in panel (a) represent the mean of measurements by van den Broeke et al., 2004 for the Stations S5, S6 and S9 during 2003-2007. The cloud effect depends on the cloud optical thickness with is parameterized by a function of elevation (full lines). The cloud effect is lower on dirty ice (dashed lines). The effect of the zenith angle of the sun (b) is zero when the sun is below the horizon and highest in spring and autumn when the zenith angles are high. The overall negative effect of high BC remains it is only weakened by the low-standing sun. For example, the darkening effect of BC ($d\alpha_c$) with 1 ppm BC is -0.40 which is reduced by the zenith angle to -0.15 in early spring and about -0.30 in mid summer.
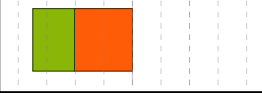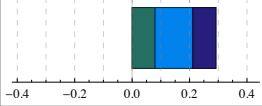
Process	Potential albedo change	Sub–process	Values	Reference
Snow impurities		BC dust	−0.04 −0.019	with 20 cm^{2}g^{-1} and 0.02 ppm BC with 20 cm^{2}g^{-1} and 1. ppm dust
Snow other		SSA: ageing zenith angle clouds	0.214 0.088 0.086	difference between 1600 and 20 cm^{2}g^{-1} with 200 cm^{2}g^{-1} and 89.9° and no impurities with 200 cm^{2}g^{-1} no BC, at S5 elevation and τ=12
Ice impurities		BC dust	−0.203 −0.146	with 2 cm^{2}g^{-1} and 0.1 ppm BC with 2 cm^{2}g^{-1} and 9. ppm dust
Ice other		SSA: cracks ... zenith angle clouds	0.08 0.132 0.08	difference between 7 and 2. cm^{2}g^{-1} with 2 cm^{2}g^{-1} and 89.9° and no impurities with 2 cm^{2}g^{-1}, no BC, at S5 elevation and τ=12
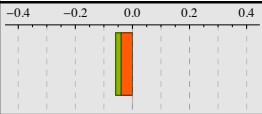
FIGURE S2. Ranges of albedo changes at the ablation zone of Greenland derived from the parameterization of Gardner and Sharp, 2010. The ranges of albedo lowering due to dust and BC in snow are low, even with high impurity loadings and very dense snow. Snow aging has the potentially biggest influence on albedo of snow. Impurities on ice have a range of about 0.35 in total, due to the low specific surface area of ice and the high impurity concentrations caused by accumulation over several years and melt-out from highly contaminated ice. In addition the zenith angle has a high, positive effect on the albedo of ice.
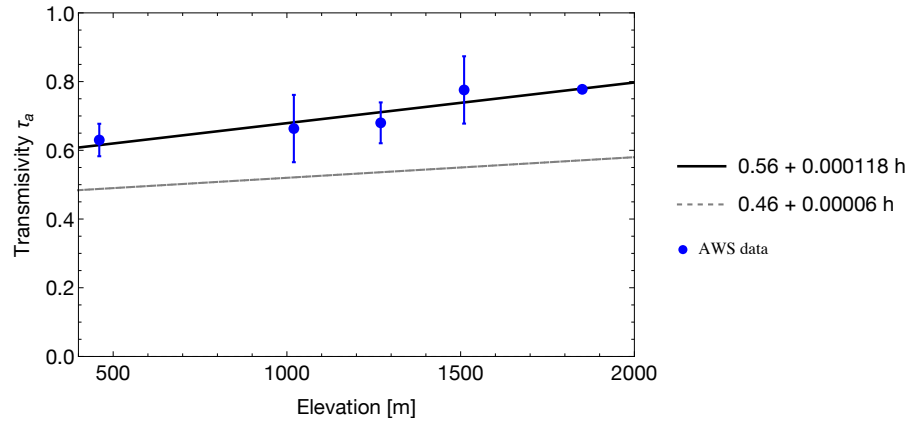
FIGURE S3. Transmissivity versus elevation with the linear fit of Robinson et al., 2010 (dashed line) and a linear fit obtained by comparing the modeled net shortwave radiation with observations for the years 2005-2012. The blue dots are calculated transmissivity values for each station with standard deviations. These values were obtained be minimizing the difference of observed net shortwave radiation and the modeled one $(\tau_a(1 - \alpha_{\rm s})S_{\rm TOA})$ with the observed albedo, see also Figure S4 below.
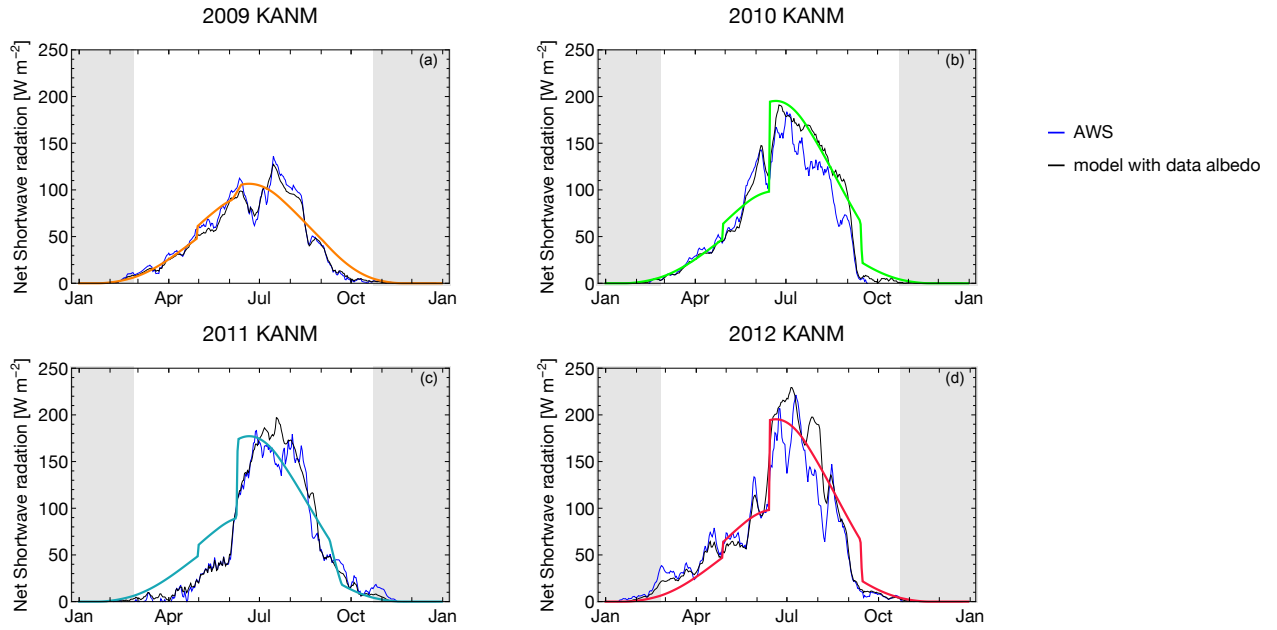
FIGURE S4. Comparison of net short wave radiation of the station KAN_M of the years 2009-2012. The grey areas indicate periods when the sun is below the horizon. The black line is the modeled net shortwave radiation $\tau_a(1 - \alpha_s)S_{\mathrm{TOA}}$ with the albedo derived from AWS measurements. The similarity between the AWS net shortwave radiation (in blue) and the black line is an indicator of the quality of the transmissivity τ_a (see Figure S3 above). The green line is the modeled net shortwave radiation with the free parameters calibrated to each year (see Figure 5 in the main text).
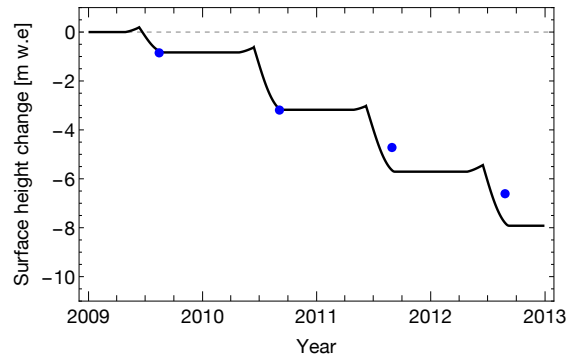
FIGURE S5. Surface height change of KAN_M with the calibrated model runs compared to data in blue from Machguth et al, submitted. The increase in surface height during spring each year is caused by superimposed ice formation.
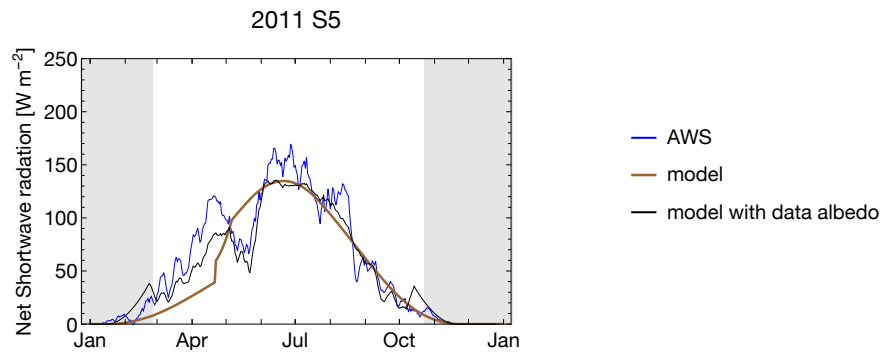

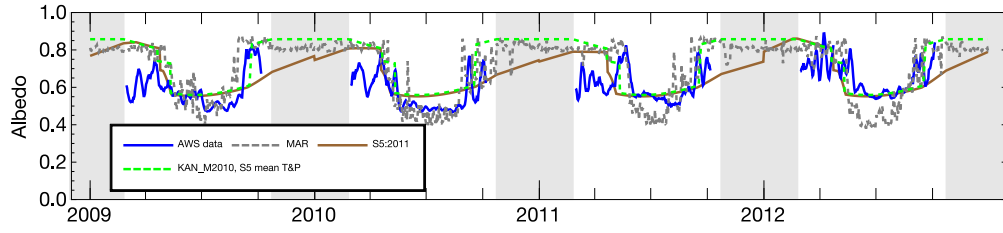FIGURE S6. Same as Figure S4, but for station S5.

FIGURE S7. Albedo data and simulation for station S5 with parameters optimized for 2011 (in brown) and the mean model configuration of KAN_M in 2010 (green) with the mean temperature and precipitation of S5 ($\overline{P}$ (1.24 10^{-8} m w.e s^{-1}), $T_{\oplus}$ (3.70°C) and ς (0.19 °C day^{-1}). The albedo data of the AWS (in blue) and of the regional climate model MAR (in dashed black) are shown for comparison and are smoothed with a moving average over a seven-day window. Grey areas indicate periods when the sun zenith angle is higher than 90°(i.e. the sun is below the horizon at mid-day).
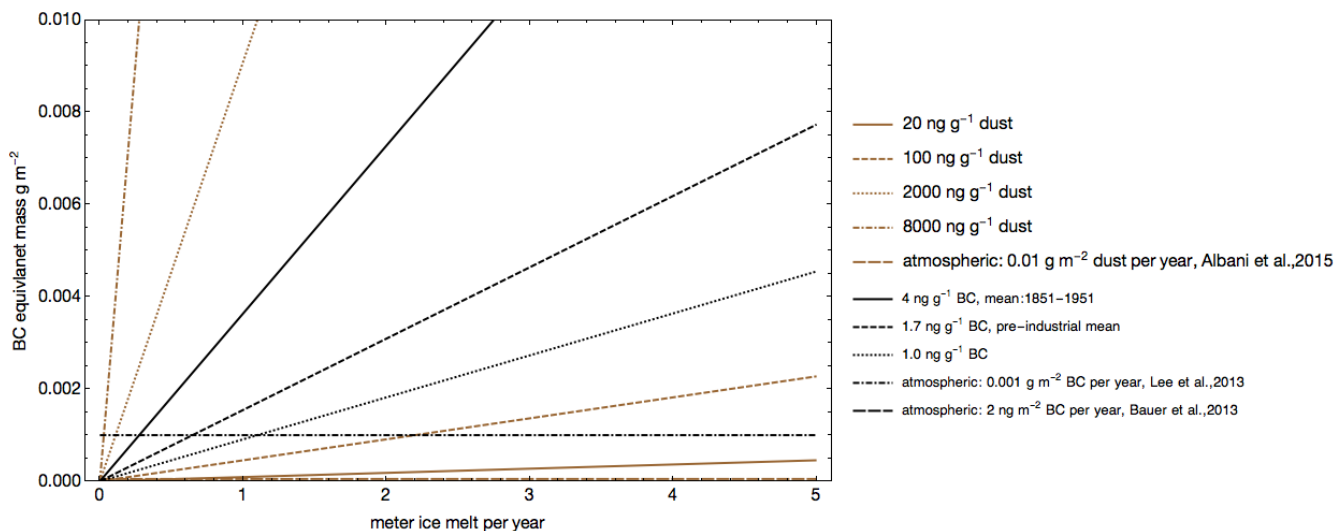
FIGURE S8. Comparison of annual melt-out and atmospheric deposition of BC (black) and dust (brown). The values of dust are converted in BC by assuming a 200 times weaker absorption. The atmospheric rate of deposition of dust is too low to be visible, therefore melt-out of dust is always the dominant source. The atmospheric deposition of BC is the dominant source when the englacial concentration is 1.0 ng g^{-1} and the annual melt below one meters. Otherwise, BC deposition is dominated by melt-out but atmospheric deposition still plays a significant role. This graph can also be used to guess which impurity is mostly responsible for lowering the ice albedo. If the concentrations of BC and dust are known then the steepest line belongs to the main contributor. For example, at S5 the BC concentration is 1.0 ng g^{-1} and the dust concentration 100 ng g^{-1}. The line of the BC concentration is steeper and therefore S5 is dominated by BC, which was also the result from the detailed simulation.

References

Albani, S., Mahowald, N. M., Winckler, G., Anderson, R. F., Bradtmiller, L. I., Delmonte, B., François, R., Goman, M., Heavens, N. G., Hesse, P. P., Hovan, S. A., Kang, S. G., Kohfeld, K. E., Lu, H., Maggi, V., Mason, J. A., Mayewski, P. A., McGee, D., Miao, X., Otto-Bliesner, B. L., Perry, A. T., Pourmand, A., Roberts, H. M., Rosenbloom, N., Stevens, T. and Sun, J.: Twelve thousand years of dust: the Holocene global dust cycle constrained by natural archives, Clim Past, 11(6), 869–903, doi:10.5194/cp-11-869-2015, 2015.

Bauer, S. E., Bausch, A., Nazarenko, L., Tsigaridis, K., Xu, B., Edwards, R., Bisiaux, M. and McConnell, J.: Historical and future black carbon deposition on the three ice caps: Ice core measurements and model simulations from 1850 to 2100,, 118(14), 7948–7961, doi:10.1002/jgrd.50612, 2013.

Gardner, A. and Sharp, M.: A review of snow and ice albedo and the development of a new physically based broadband albedo parameterization, Journal of Geophysical Research, 115(F1), F01009, doi:10.1029/2009JF001444, 2010.

Lee, Y. H., Lamarque, J. F., Flanner, M. G., Jiao, C., Shindell, D. T., Berntsen, T., Bisiaux, M. M., Cao, J., Collins, W. J., Curran, M., Edwards, R., Faluvegi, G., Ghan, S., Horowitz, L. W., McConnell, J. R., Ming, J., Myhre, G., Nagashima, T., Naik, V., Rumbold, S. T., Skeie, R. B., Sudo, K., Takemura, T., Thevenon, F., Xu, B. and Yoon, J. H.: Evaluation of preindustrial to present-day black carbon and its albedo forcing from Atmospheric Chemistry and Climate Model Intercomparison Project (ACCMIP), Atmos. Chem. Phys., 13(5), 2607–2634, doi:10.5194/acp-13-2607-2013, 2013.

Machguth, H., H.H. Thomsen, A. Weidick, J. Abermann, A.P. Ahlstrøm, M. L. Andersen, S.B. Andersen, A. A. Bjørk, J. E. Box, R. J. Braithwaite, C.E. Bøggild, M. Citterio, P. Clement, W. Colgan, R. S. Fausto, K. Gleie, B. Hasholt, B. Hynek, N.T. Knudsen, S.H. Larsen, S. Mernild, J. Oerlemans, H. Oerter, O.B. Olesen, C.J.P.P. Smeets, K. Steffen, M. Stober, S. Sugiyama D. van As, M.R. van den Broeke and R. S. van de Wal (submitted): Greenland surface mass balance observations from the ice sheet ablation area and local glaciers, J. Glaciol.

Robinson, A., Calov, R. and Ganopolski, A.: An efficient regional energy-moisture balance model for simulation of the Greenland Ice Sheet response to climate change, The Cryosphere, 4(2), 129–144, doi:10.5194/tc-4-129-2010, 2010.

Van As, D., Hubbard, A. L., Hasholt, B., Mikkelsen, A. B., van den Broeke, M. R. and Fausto, R. S.: Large surface meltwater discharge from the Kangerlussuaq sector of the Greenland ice sheet during the record-warm year 2010 explained by detailed energy balance observations, The Cryosphere, 6(1), 199–209, doi:10.5194/tc-6-199-2012, 2012.

Van den Broeke, M. R., Smeets, P., Ettema, J. and Munneke, P. K.: Surface radiation balance in the ablation zone of the west Greenland ice sheet, Journal of Geophysical Research, 113(D13), D13105, 2008.